Chu *et al. EURASIP Journal on Wireless Communications and Networking* (2016) 2016:244
DOI 10.1186/s13638-016-0700-7

EURASIP Journal on Wireless Communications and Networking

RESEARCH Open Access

Hybrid spectrum access with relay assisting both primary and secondary networks under imperfect spectrum sensing

Thi My Chinh Chu[1*], Hans-Jürgen Zepernick[1] and Hoc Phan[2]

Abstract

This paper proposes a novel hybrid interweave-underlay spectrum access for a cognitive amplify-and-forward relay network where the relay forwards the signals of both the primary and secondary networks. In particular, the secondary network (SN) opportunistically operates in interweave spectrum access mode when the primary network (PN) is sensed to be inactive and switches to underlay spectrum access mode if the SN detects that the PN is active. A continuous-time Markov chain approach is utilized to model the state transitions of the system. This enables us to obtain the probability of each state in the Markov chain. Based on these probabilities and taking into account the impact of imperfect spectrum sensing of the SN, the probability of each operation mode of the hybrid scheme is obtained. To assess the performance of the PN and SN, we derive analytical expressions for the outage probability, outage capacity, and symbol error rate over Nakagami-*m* fading channels. Furthermore, we present comparisons between the performance of underlay cognitive cooperative radio networks (CCRNs) and the performance of the considered hybrid interweave-underlay CCRN in order to reveal the advantages of the proposed hybrid spectrum access scheme. Eventually, with the assistance of the secondary relay, performance improvements for the PN are illustrated by means of selected numerical results.

Keywords: Cognitive radio network, Continuous-time Markov chain, Hybrid spectrum access, Amplify-and-forward, Relay networks, Nakagami-*m* fading

1 Introduction

In recent years, the growing demand of mobile multimedia services has led to a serious shortage of radio frequency spectrum. However, measurement campaigns have shown that most of the allocated spectrum bands are underutilized [1]. To alleviate the severe scarcity of spectrum resources, a promising technique, called cognitive radio, has been developed. This technology allows secondary users (SUs) to access the licensed spectrum of the primary users (PUs) by utilizing interweave, underlay, or overlay spectrum access techniques [2–4]. In particular, in the interweave spectrum access, the SU periodically monitors the radio spectrum to detect occupancy in the different parts of the spectrum and then opportunistically utilizes the spectrum holes for its communication [4]. A drawback of this scheme is the limitation on access time which leads to a reduction in the effectiveness of spectrum utilization compared to other spectrum access schemes. However, an interweave cognitive radio network (CRN) may achieve high performance since the transmit power of the secondary transmitter is not bounded by the interference power constraint of the primary receiver. In the overlay spectrum access, the SU is only allowed to access frequency bands if the secondary network (SN) uses interference cancelation techniques to mitigate interference to the primary network (PN) [2]. In the underlay spectrum access, the PU and SU can concurrently operate in the same licensed spectrum, but the secondary transmitter must adjust its transmit power to meet the interference power constraint of the primary receiver [3]. Due to this interference power constraint, the SUs have to reduce their transmit powers which degrades the performance of the SN. To reveal the performance of CRNs using different spectrum access schemes, comparisons of the

*Correspondence: thi.my.chinh.chu@bth.se
[1]Blekinge Institute of Technology, SE-371 79 Karlskrona, Sweden
Full list of author information is available at the end of the article

outage probability for CRNs using interweave, underlay, and overlay techniques were presented in [5].

Inspired by the inherent benefits of the overlay and underlay spectrum access, hybrid overlay-underlay CRNs have been proposed in [6, 7]. Specifically, Oh and Choi [6] derived the optimal switching rate between spectrum access modes in order to maximize throughput of a hybrid overlay-underlay CRN. A power allocation strategy for a hybrid overlay-underlay CRN was proposed in [7] to maximize the channel capacity of the CRN. The works of [8, 9] focused on incorporating cooperative communications into hybrid overlay-underlay CRNs to benefit from both the cognitive radio and cooperative communication techniques such as efficient spectrum utilization and improved link reliability, respectively. In [10], a novel hybrid scheme which combines the interweave and underlay schemes for a single hop CRN was introduced. Specifically, an M/M/1 queuing model with Poisson traffic arrival is utilized in [10] to analyze the average service rate of video services for a hybrid interweave-underlay CRN. In [11], the spectrum access of a hybrid interweave-underlay cognitive cooperative radio network (CCRN) was modeled as a continuous-time Markov chain (CTMC) to obtain the steady state probabilities of the interweave and underlay modes. Nevertheless, the relay in [11] only forwards the signals of the secondary network but does not support the primary network. Recently, in [12], an amplify-and-forward (AF) relay has been employed to forward the signals of both the primary and secondary networks which provides a performance gain for the PN as well as an improved spectrum utilization. However, the SUs of the CCRN in [12] utilize the underlay spectrum access under the interference constraint of the PUs all the time regardless of the activity of the PUs. To the best of our knowledge, no work has deployed hybrid interweave-underlay spectrum access for CCRNs where the relay forwards the signals of the PNs and SNs in which the effect of imperfect spectrum sensing is considered.

In this paper, we examine a hybrid interweave-underlay spectrum access scheme for CCRNs. The motivation for this kind of hybrid spectrum access scheme is to inherent benefits of both the underlay and interweave spectrum access schemes. Specifically, the CCRN basically operates in the underlay spectrum access to obtain high spectrum efficiency, i.e., if the CCRN senses that it is concurrently active with the PN, the SUs must operate in the underlay spectrum access. In this operation mode, the SUs must control their transmit powers to satisfy the interference power constraint. However, if the PN is sensed to be inactive, the SUs opportunistically operate in the interweave mode without facing the interference power constraint imposed by the primary receiver to improve the system performance. In order to benefit from the advantages of relaying communication, in our proposed scheme, the secondary relay forwards the signals of the PN and CCRN. This is different from overlay CCRNs where the SUs have knowledge of the codebook of the PU and utilize this information to decode the message of primary users [2]. In our system, the secondary relay simply amplifies the signals of the PN and CCRN and broadcasts the resulting signals. It is noted that, in our study, the characteristics of traffic patterns of the PUs and SUs are taken into account when modeling the spectrum access. Further, the impact of imperfect spectrum sensing of the SUs are also considered when analyzing the system performance of the PN and SN. It is assumed that the PN and SN are subject to Nakagami-m fading. The Nakagami-m fading model is used here as it comprises a wide variety of fading channels as special cases by setting the fading severity parameter m to particular values. For example, $m = 0.5$ represents one-sided Gaussian fading and $m = 1$ represents Rayleigh fading. The Nakagami-m fading model also closely approximates the Nakagami-q (Hoyt) and the Nakagami-n (Rice) models.

Our proposed novel hybrid interweave-underlay spectrum access for a CCRN where the relay forwards the signals of both the primary and secondary networks aims at two goals, i.e., improving spectrum efficiency and enhancing performance for both the PN and SN. Major contributions of this paper can be summarized as follows:

- We develop a CTMC to model the spectrum access of a hybrid interweave-underlay CCRN wherein the secondary AF relay assists primary and secondary communications.
- On this basis, the equilibrium probability of each operation mode of the hybrid interweave-underlay CCRN over Nakagami-m fading is derived.
- The effect of imperfect spectrum sensing in terms of false alarm and missed detection of the CCRN on the system performance is also investigated.
- We further develop an analytical framework to assess the performance of the secondary and primary networks in terms of outage probability, outage capacity, and symbol error rate.
- We also make performance comparisons between the proposed hybrid CCRN and the conventional underlay CCRN to reveal the superior performance of the hybrid CCRN.
- Finally, through the provided numerical results, essential insights into the impact of network parameters on system performance are revealed.

The rest of this paper is organized as follows. Section 2 describes the system model, constructs the CTMC, and calculates the probabilities of operation modes in the PN and SN. Sections 3, 4, and 5 derive the expressions for outage probability, outage capacity, and symbol error rate

(SER) for the PN and SN, respectively. Selected numerical results are provided in Section 6. Finally, conclusions are given in Section 7.

Notation: We use the following notations in the paper. $\Gamma(n)$ and $\Gamma(n,x)$ are the gamma function ([13], Eq. (8.310.1)) and incomplete gamma function ([13], Eq. (8.350.2)), respectively. The nth order modified Bessel function of the second kind is denoted as $\mathcal{K}_n(\cdot)$ ([13], Eq. (8.432.1)) and $U(a,b;x)$ is the confluent hypergeometric function ([13], Eq. (9.211.4)). Moreover, ${}_2F_1(\alpha,\beta;\gamma;z)$ is the Gauss hypergeometric function ([13], Eq. (9.100)). Further, $E\{\cdot\}$ stands for the expectation operator and $C_n^k = k!/[\,n!\,(k-n)!\,]$ denotes the binomial coefficient. Finally, the probability density function (PDF) and the cumulative distribution function (CDF) of a random variable (RV) X are denoted as $f_X(\cdot)$ and $F_X(\cdot)$, respectively. For Nakagami-m fading with fading severity parameter m_i, channel mean power Ω_i, and $\alpha_i = m_i/\Omega_i$, the PDF and CDF of the channel power gain X_i are expressed as [14]

$$f_{X_i}(x_i) = \frac{\alpha_i^{m_i}}{\Gamma(m_i)} x_i^{m_i-1} \exp(-\alpha_i x_i) \tag{1}$$

$$F_{X_i}(x_i) = 1 - \exp(-\alpha_i x_i) \sum_{j=0}^{m_i-1} \frac{\alpha_i^j x_i^j}{j!} \tag{2}$$

2 System and channel model

We consider a cognitive AF relay network consisting of a secondary transmitter SU_{TX}, AF relay SU_R, secondary receiver SU_{RX}, primary transmitter PU_{TX}, and primary receiver PU_{RX} (see Fig. 1). In this network, we denote $h_1, h_2, h_3, h_4, h_5, h_6, h_7$, and h_8 as the channel coefficients of the links $PU_{TX} \to SU_R, SU_R \to PU_{RX}, PU_{TX} \to PU_{RX}, SU_{TX} \to SU_R, SU_R \to SU_{RX}, SU_{TX} \to SU_{RX}, SU_{TX} \to PU_{RX}$, and $PU_{TX} \to SU_{RX}$, respectively. Furthermore, corresponding to the notation of the channel coefficients, let d_1, d_2, d_3, d_4, d_5, d_6, d_7, and d_8 be the normalized distances of the respective links. Assume that the relay forwards the signals of the PN and SN and that both networks are subject to Nakagami-m fading. It is also assumed that the PN and SN share the same spectrum by utilizing a hybrid interweave-underlay scheme. Before transmitting the signals, the SUs must sense the channel to identify whether the PN is active or not. If the PN is active, the SUs must operate in the underlay mode where SU_{TX} and SU_R must control their transmit powers subject to the interference power threshold Q of PU_{RX}. On the contrary, if the PN is inactive, SU_{TX} and SU_R switch to the interweave mode and can send the signals up to the transmit power limit.

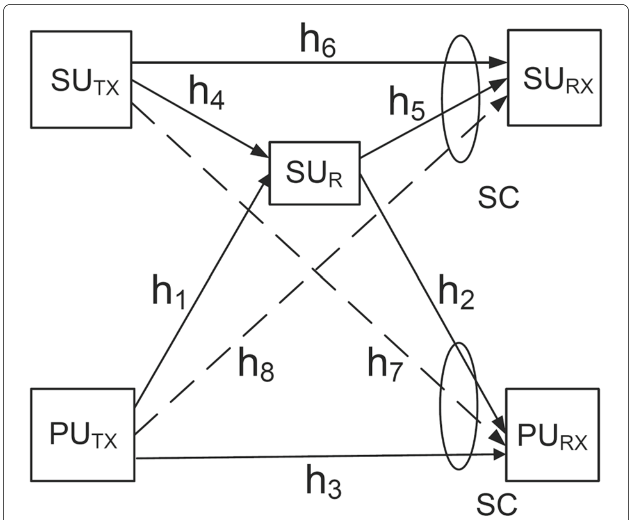

Fig. 1 System model of the hybrid CCRN (SC = selection combining)

Let the arrival traffics of PU_{TX} and SU_{TX} be modeled as Poisson processes with arrival rates λ_p and λ_s, respectively. Further, the departure traffics of PU_{TX} and SU_{TX} are also Poisson processes with departure rates μ_p and μ_s, respectively. Since relaying transmission is deployed, departure traffics of PU_{TX} and SU_{TX} become arrival traffics of SU_R with rates μ_p and μ_s, respectively. Finally, the departure traffics at SU_R resulting from the arrival traffics of PU_{TX} and SU_{TX} are also Poisson processes with rates μ_r^p and μ_r^s, respectively. As a result, when the PN and SN are concurrently active, the arrival of the system is $\lambda_p + \lambda_s$. Further, the arrival and departure rates of SU_R are $\mu_p + \mu_s$ and $\mu_r^s + \mu_r^p$, respectively.

In this system, the communication occurs over two time slots. In the first time slot, PU_{TX} and/or SU_{TX} transmit their signals to the relay. The relay SU_R amplifies and then forwards the signals to the destinations in the second time slot, i.e., the event that both PU_{TX} and SU_R or both SU_{TX} and SU_R simultaneously transmit signals never occurs. Thus, we can model the spectrum access of the system as the seven-state transition diagram shown in Fig. 2. In Fig. 2, State 0 represents the event that all terminals, PU_{TX}, SU_{TX}, and SU_R, are inactive. Furthermore, States P, S, and PS correspond to the events that only PU_{TX}, only SU_{TX}, and both PU_{TX} and SU_{TX} are active, respectively. Finally, States R^P, R^S, and R stand for the events that SU_R forwards the signal of only the PU_{TX}, of only the SU_{TX}, and of both the PU_{TX} and SU_{TX}, respectively.

Given the state transition diagram of the CTMC shown in Fig. 2, we construct a linear equation system consisting of the flow-balance equations and the normalized equation. This enables us to obtain the steady state probability of each state. In this equation system, a flow-balance equation represents the law that the arrival rate of any state is always equal to its departure rate. Furthermore, the normalized equation expresses the fact that the sum of all steady state probabilities is always equal

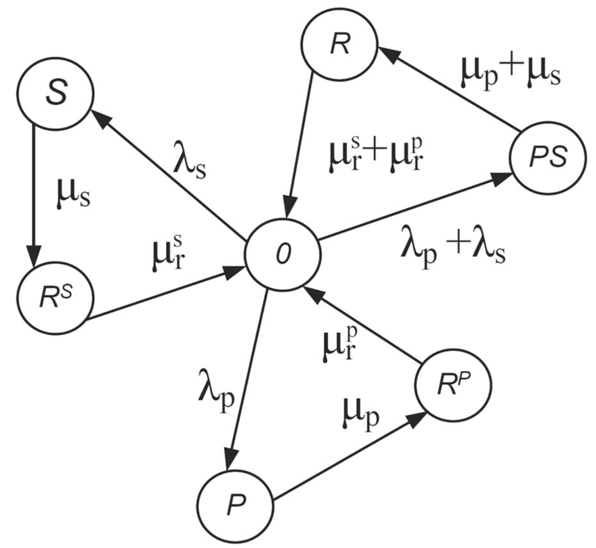

Fig. 2 State transaction diagram of the continuous-time Markov chain

to one. As a result, the linear equation system is given as follows:

$$\begin{aligned}\mu_r^s P_{R^S} + \left(\mu_r^s + \mu_r^p\right) P_R + \mu_r^p P_{R^P} &= 2(\lambda_s + \lambda_p) P_0\\ \lambda_s P_0 &= \mu_s P_S\\ \mu_s P_S &= \mu_r^s P_{R^S}\\ (\mu_s + \mu_p) P_{PS} &= \left(\mu_r^s + \mu_r^p\right) P_R\\ \mu_p P_P &= \mu_r^p P_{R^P}\\ \lambda_p P_0 &= \mu_p P_P\\ (\lambda_s + \lambda_p) P_0 &= (\mu_p + \mu_s) P_{PS}\\ P_0 + P_S + P_{R^S} + P_R + P_{R^P} + P_P + P_{PS} &= 1\end{aligned} \tag{3}$$

where $P_0, P_P, P_S, P_{PS}, P_R, P_{R^S}$, and P_{R^P} are the probabilities that the system resides in State 0, State P, State S, State PS, State R, State R^S, and State R^P, respectively. Since there exist seven system states, it is sufficient to select six independent balance equations and the normalized equation from (3) to obtain the seven steady state probabilities. Therefore, we can rewrite the set of the first six flow-balance equations and the normalized equation as $\mathbf{Ap} = \mathbf{b}$ where $\mathbf{p}$ and $\mathbf{b}$ are vectors defined as $\mathbf{b} = (0000001)^T$ and $\mathbf{p} = \left(P_0 P_S P_{R^S} P_R P_{R^P} P_P P_{PS}\right)^T$. Furthermore, $\mathbf{A}$ is a 7×7 matrix constructed as

$$\mathbf{A} = \begin{bmatrix} -2\left(\lambda_s + \lambda_p\right) & 0 & \mu_r^s & \left(\mu_r^s + \mu_r^p\right) & \mu_r^p & 0 & 0\\ \lambda_s & -\mu_s & 0 & 0 & 0 & 0 & 0\\ 0 & \mu_s & -\mu_r^s & 0 & 0 & 0 & 0\\ 0 & 0 & 0 & -\left(\mu_r^s + \mu_r^p\right) & 0 & 0 & (\mu_s + \mu_p)\\ 0 & 0 & 0 & 0 & -\mu_r^p & \mu_p & 0\\ \lambda_p & 0 & 0 & 0 & 0 & -\mu_p & 0\\ 1 & 1 & 1 & 1 & 1 & 1 & 1 \end{bmatrix} \tag{4}$$

Then, the vector $\mathbf{p}$, consisting of the seven steady state probabilities, is obtained as

$$\mathbf{p} = \mathbf{A}^{-1}\mathbf{b} \tag{5}$$

Let p_p and p_s be the probabilities that the PN and the CCRN are active, respectively. Then, p_p and p_s are calculated as

$$p_p = P_P P_{R^P} + P_{PS} P_R \tag{6}$$

$$p_s = P_S P_{R^S} + P_{PS} P_R \tag{7}$$

When considering the impact of imperfect spectrum sensing at the SUs, the missed detection and false alarm probabilities must be taken into account. The missed detection probability, p_m, is the probability that the SUs consider the licensed spectrum as being vacant although it is occupied by the PU. False alarm probability, p_f, is the probability that the SUs consider the licensed spectrum as occupied by the PU even though the PU is inactive. Then, the detection probability and no false alarm probability can be calculated from the missed detection and false alarm probabilities as $(1 - p_m)$ and $(1 - p_f)$, respectively. Taking into account imperfect spectrum sensing, the following scenarios of the PN and CCRN can occur depending on the states of the terminals in the networks.

2.1 Scenario 1: The secondary network operates in underlay mode

In this scenario, the SUs sense that the spectrum band is occupied by the PN. Therefore, the SUs must operate in underlay mode under the interference power constraint Q imposed by the $\mathrm{PU_{RX}}$, i.e., $\mathrm{SU_{TX}}$ transmits the signal $x_s^{(1)}$ with average power $P_s^{(1)} = Q/|h_7|^2$ where h_7 is the channel coefficient from $\mathrm{SU_{TX}}$ to $\mathrm{PU_{RX}}$. Further, the amplifying gain G_1 at $\mathrm{SU_R}$ is selected to guarantee that the interference from the CCRN to the primary receiver does not go beyond Q, i.e.,

$$G_1^2 = |h_7|^2/(|h_2|^2|h_4|^2) \tag{8}$$

There are two cases that Scenario 1 occurs.

- *Case 1*: The PN and SN are active and the SN correctly senses the active state of the PN. The probability of this event is

$$p_p^{(1,1)} = p_s^{(1,1)} = (1 - p_m) P_{PS} P_R \tag{9}$$

  The communication in Case 1 is described as follows. In the first time slot, $\mathrm{PU_{TX}}$ and $\mathrm{SU_{TX}}$ broadcast their signals to the relay and to their respective receivers, $\mathrm{PU_{RX}}$ and $\mathrm{SU_{RX}}$. Since the PN and SN concurrently share the same spectrum, $\mathrm{SU_{TX}}$ must control its transmit power subject to the interference power threshold Q. As a result, the received signal $y_{1p}^{(1,1)}$ at $\mathrm{PU_{RX}}$, the received signal $y_{1s}^{(1,1)}$ at $\mathrm{SU_{RX}}$, and the received signal $y_r^{(1,1)}$ at $\mathrm{SU_R}$ in the first time slot are, respectively, given by

$$y_{1p}^{(1,1)} = h_3 x_p + h_7 x_s^{(1)} + n_p \tag{10}$$

$$y_{1s}^{(1,1)} = h_6 x_s^{(1)} + h_8 x_p + n_s \tag{11}$$

$$y_r^{(1,1)} = h_1 x_p + h_4 x_s^{(1)} + n_r \tag{12}$$

where x_p is the transmit signal at $\mathrm{PU_{TX}}$ with average power P_p. Further, n_p, n_s, and n_r denote the additive white Gaussian noise (AWGN) with zero mean and variance N_0 at $\mathrm{PU_{RX}}, \mathrm{SU_{RX}}$, and $\mathrm{SU_R}$, respectively. As for the received signal at the relay, the term $h_4 x_s^{(1)}$ in (12) can be considered as interference from the SN to the PN and the term $h_1 x_p$ can be considered as the interference from the PN to the SN. Usually, these terms are much larger than the noise term n_r, such that n_r in (12) can be neglected as suggested in [15].

In the second time slot, $\mathrm{SU_R}$ amplifies the received signal $y_r^{(1,1)}$ with the gain G_1 and then forwards the primary and secondary signals. Consequently, the received signal $y_{2p}^{(1,1)}$ at $\mathrm{PU_{RX}}$ and the received signal $y_{2s}^{(1,1)}$ at $\mathrm{SU_{RX}}$ in the second time slot are, respectively, given by

$$y_{2p}^{(1,1)} = G_1 h_1 h_2 x_p + G_1 h_2 h_4 x_s^{(1)} + n_p \tag{13}$$

$$y_{2s}^{(1,1)} = G_1 h_1 h_5 x_p + G_1 h_4 h_5 x_s^{(1)} + n_s \tag{14}$$

Assume that $\mathrm{PU_{RX}}$ and $\mathrm{SU_{RX}}$ deploy selection combining (SC) to select the best signal among the direct link and relaying link. From (10) and (13), the instantaneous signal-to-interference-plus-noise ratio (SINR) of the PN is obtained as

$$\gamma_p^{(1,1)} = \max\left[\gamma_{1p}^{(1,1)}, \gamma_{2p}^{(1,1)}\right] \tag{15}$$

where $\gamma_{1p}^{(1,1)}$ and $\gamma_{2p}^{(1,1)}$ are, respectively, the instantaneous SINRs of the direct link and relaying link of the PN, i.e.,

$$\gamma_{1p}^{(1,1)} = X_3/(\beta_1 + \beta_2) \tag{16}$$

$$\gamma_{2p}^{(1,1)} = X_1 X_7/[(\beta_1 + \beta_2) X_4] \tag{17}$$

Here, $\beta_1 = Q/P_p$, $\beta_2 = N_0/P_p$, and $X_l = |h_l|^2$, $l = 1, 2, \ldots, 8$. From (11) and (14), the instantaneous SINR of the direct link $\gamma_{1s}^{(1,1)}$ and relaying link $\gamma_{2s}^{(1,1)}$ of the SN are, respectively, given by

$$\gamma_{1s}^{(1,1)} = \beta_1 X_6/[X_7 X_8 + \beta_2 X_7] \tag{18}$$

$$\gamma_{2s}^{(1,1)} = \beta_1 X_4 X_5/[X_1 X_5 X_7 + \beta_2 X_2 X_4] \tag{19}$$

Thus, the instantaneous SINR of the SN is obtained as

$$\gamma_s^{(1,1)} = \max\left[\gamma_{1s}^{(1,1)}, \gamma_{2s}^{(1,1)}\right] \tag{20}$$

- *Case 2*: The PN is inactive but the SN senses that the PN is active. The probability of this event is

$$p_s^{(1,2)} = p_f P_S P_{R^S} \tag{21}$$

Though the PN is inactive, due to the false alarm, $\mathrm{SU_{TX}}$ senses the PN as active and still controls its transmit power $P_s^{(1)}$ subject to Q. As a result, the received signal $y_{1s}^{(1,2)}$ at $\mathrm{SU_{RX}}$, and the received signal $y_r^{(1,2)}$ at $\mathrm{SU_R}$ in the first time slot are, respectively, given by

$$y_r^{(1,2)} = h_4 x_s^{(1)} + n_r \tag{22}$$

$$y_{1s}^{(1,2)} = h_6 x_s^{(1)} + n_s \tag{23}$$

In the second time slot, $\mathrm{SU_R}$ amplifies the received signal with the gain G_1 and then forwards the resulting signal. Hence, the received signal at $\mathrm{SU_{RX}}$ in the second time slot is given by

$$y_{2s}^{(1,2)} = G_1 h_5 h_4 x_s^{(1)} + G_1 h_5\, n_r + n_s \tag{24}$$

Considering the instantaneous signal-to-noise ratio as a particular case of SINR where no interference exists, the SINR of the CCRN is obtained from (23) and (24) as

$$\gamma_s^{(1,2)} = \max\left[\gamma_{1s}^{(1,2)}, \gamma_{2s}^{(1,2)}\right] \tag{25}$$

where $\gamma_{1s}^{(1,2)}$ and $\gamma_{2s}^{(1,2)}$ are, respectively, the instantaneous SINRs of the direct link and the relaying link of the SN, i.e.,

$$\gamma_{1s}^{(1,2)} = \beta_1 X_6/(\beta_2 X_7) \tag{26}$$

$$\gamma_{2s}^{(1,2)} = \beta_1 X_4 X_5/[\beta_2 (X_5 X_7 + X_2 X_4)] \tag{27}$$

2.2 Scenario 2: The secondary network operates in interweave mode

In this scenario, the SUs sense that the PN is inactive. Thus, the SUs operate in interweave mode and the SN does not consider the interference power constraint Q of the PN. Then, $\mathrm{SU_{TX}}$ transmits the signal $x_s^{(2)}$ with average power P_s. Further, the gain factor G_2 at $\mathrm{SU_R}$ is selected to guarantee that the transmit powers at $\mathrm{SU_{TX}}$ and $\mathrm{SU_R}$ are the same, i.e, G_2 is selected as

$$G_2^2 = 1/|h_4|^2 \tag{28}$$

There are two cases that cause Scenario 2 to happen.

- *Case 1*: Only the SN is active and the inactive state of the PN is correctly sensed. The probability of this event is

$$p_s^{(2,1)} = (1 - p_f) P_S P_{R^S} \tag{29}$$

Since the SUs sense that the PN is inactive, the SN operates in interweave mode without suffering from the interference power constraint of $\mathrm{PU_{RX}}$. Furthermore, there is no interference incurred by the PN to the SN. As a result, the received signal $y_r^{(2,1)}$ at SU_R and the received signal $y_{1s}^{(2,1)}$ at SU_{RX} in the first time slot are, respectively, given by

$$y_r^{(2,1)} = h_4 x_s^{(2)} + n_r \tag{30}$$

$$y_{1s}^{(2,1)} = h_6 x_s^{(2)} + n_s \tag{31}$$

In the second time slot, SU_R amplifies the received signal $y_r^{(2,1)}$ with the gain G_2 and then forwards the resulting signal to SU_{RX}. Thus, the received signal $y_{2s}^{(2,1)}$ at SU_{RX} in the second time slot can be expressed as

$$y_{2s}^{(2,1)} = G_2 h_5 h_4 x_s^{(2)} + G_2 h_5\, n_r + n_s \tag{32}$$

Defining $\beta_3 = P_s/N_0$, the instantaneous SINRs of the direct link $\gamma_{1s}^{(2,1)}$ and relaying link $\gamma_{2s}^{(2,1)}$ of the SN are, respectively, obtained from (31) and (32) as

$$\gamma_{1s}^{(2,1)} = \beta_3 X_6 \tag{33}$$

$$\gamma_{2s}^{(2,1)} = \beta_3 X_4 X_5/(X_4 + X_5) \tag{34}$$

Thus, the instantaneous SINR of the SN is obtained as

$$\gamma_s^{(2,1)} = \max\left[\gamma_{1s}^{(2,1)}, \gamma_{2s}^{(2,1)}\right] \tag{35}$$

- *Case 2*: Both the PN and SN are active but the SN senses that the PN is inactive. With the incorrect sensing outcome, the SN operates in interweave mode though the PN is active. The probability of this event is

$$p_p^{(2,2)} = p_s^{(2,2)} = p_m P_{PS} P_R \tag{36}$$

Then, the PU_{TX} and SU_{TX} transmit the signals x_p and $x_s^{(2)}$ to the relay and to their respective receivers. As a result, the received signal $y_{1p}^{(2,2)}$ at PU_{RX}, the received signal $y_{1s}^{(2,2)}$ at SU_{RX}, and the received signal $y_r^{(2,2)}$ at SU_R in the first time slot are, respectively, given by

$$y_{1p}^{(2,2)} = h_3 x_p + h_7 x_s^{(2)} + n_s \tag{37}$$

$$y_{1s}^{(2,2)} = h_6 x_s^{(2)} + h_8 x_p + n_s \tag{38}$$

$$y_r^{(2,2)} = h_1 x_p + h_4 x_s^{(2)} + n_r \tag{39}$$

Again, the term $h_4 x_s^{(2)}$ in (39) represents interference from the SN to the PN while the term $h_1 x_p$ can be considered as the interference from the PN to the SN. Usually, these terms are much larger than the noise term n_r, such that n_r in (39) can be neglected [15]. As a result, the received signals, $y_{2p}^{(2,2)}$ at PU_{RX} and $y_{2s}^{(2,2)}$ at SU_{RX}, in the second time slot are, respectively, given by

$$y_{2p}^{(2,2)} = G_2 h_1 h_2 x_p + G_2 h_2 h_4 x_s^{(2)} + n_s \tag{40}$$

$$y_{2s}^{(2,2)} = G_2 h_1 h_5 x_p + G_2 h_4 h_5 x_s^{(2)} + n_s \tag{41}$$

From (37) and (40), the instantaneous SINR of the PN is obtained as

$$\gamma_p^{(2,2)} = \max\left[\gamma_{1p}^{(2,2)}, \gamma_{2p}^{(2,2)}\right] \tag{42}$$

where $\gamma_{1p}^{(2,2)}$ and $\gamma_{2p}^{(2,2)}$ are, respectively, the instantaneous SINRs of the direct and relaying links of the PN:

$$\gamma_{1p}^{(2,2)} = X_3/(\beta_2\beta_3 X_7 + \beta_2) \tag{43}$$

$$\gamma_{2p}^{(2,2)} = X_1 X_2/(\beta_2\beta_3 X_2 X_4 + \beta_2 X_4) \tag{44}$$

From (38) and (41), the instantaneous SINR of the SN is obtained as

$$\gamma_s^{(2,2)} = \max\left[\gamma_{1s}^{(2,2)}, \gamma_{2s}^{(2,2)}\right] \tag{45}$$

where $\gamma_{1s}^{(2,2)}$ and $\gamma_{2s}^{(2,2)}$ are, respectively, the instantaneous SINRs of the direct link and the relaying link of the SN, i.e.,

$$\gamma_{1s}^{(2,2)} = \beta_2\beta_3 X_6/(X_8 + \beta_2) \tag{46}$$

$$\gamma_{2s}^{(2,2)} = \beta_2\beta_3 X_4 X_5/(X_1 X_5 + \beta_2 X_4) \tag{47}$$

2.3 Scenario 3: Only the PN is active

In this scenario, the SN does not transmit and the probability of this case does not depend on the sensing outcome, i.e.,

$$p_p^{(3,1)} = P_p P_{R^P} \tag{48}$$

Hence, the received signal $y_r^{(3,1)}$ at SU_R and the received signal $y_{1p}^{(3,1)}$ at PU_{RX} in the first time slot are, respectively, given by

$$y_r^{(3,1)} = h_1 x_p + n_r \tag{49}$$

$$y_{1p}^{(3,1)} = h_3 x_p + n_p \tag{50}$$

In the second time slot, SU_R amplifies the received signal with factor $G_3^2 = 1/|h_1|^2$ to guarantee that the transmit powers of PU_{TX} and SU_R are the same. Then, SU_R forwards the resulting signal to PU_{RX}. As a result, the received signal $y_{2p}^{(3,1)}$ at PU_{RX} in the second time slot is given by

$$y_{2p}^{(3,1)} = G_3 h_2 h_1 x_p + G_3 h_2 n_r + n_p \tag{51}$$

From (50) and (51), the instantaneous SINR of the PN is given by

$$\gamma_p^{(3,1)} = \max\left[\gamma_{1p}^{(3,1)}, \gamma_{2p}^{(3,1)}\right] \tag{52}$$

where $\gamma_{1p}^{(3,1)}$ and $\gamma_{2p}^{(3,1)}$ are, respectively, the instantaneous SINRs of the direct link and the relaying link of the PN, i.e.,

$$\gamma_{1p}^{(3,1)} = X_3/\beta_2 \tag{53}$$

$$\gamma_{2p}^{(3,1)} = X_1 X_2/[\,(X_1 + X_2)\beta_2] \tag{54}$$

3 Outage probability

In order to evaluate the performance of the PN and CCRN for a given metric B, we need to first formulate the performance $B(S_i)$ for each operation mode S_i of the hybrid scheme. Then, the expectation $\overline{B}$ of B can be calculated as [16]

$$\overline{B} = \sum_{S_i \in \mathcal{S}} B(S_i) p_i \tag{55}$$

where $\mathcal{S}$ is the state space containing all operation modes, S_i is the ith operation mode, and p_i is the probability that the system operates in the ith mode. Equation (55) will be utilized in the sequel to analyze the performance of the PN and SN in terms of outage probability, outage capacity, and symbol error rate.

3.1 Outage probability of the PN

Outage probability is the probability that the instantaneous SINR falls below a predefined threshold γ_{th}. From (55), the outage probability of the PN, P_{out}^{p}, can be formulated as

$$P_{\text{out}}^{p} = \frac{p_p^{(1,1)} P_{p,\text{out}}^{(1,1)} + p_p^{(2,2)} P_{p,\text{out}}^{(2,2)} + p_p^{(3,1)} P_{p,\text{out}}^{(3,1)}}{p_p} \tag{56}$$

where $P_{p,\text{out}}^{(i,j)}$ is the outage probability of the PN in Scenario i-Case j, i.e., $P_{p,\text{out}}^{(i,j)} = F_{\gamma_p^{(i,j)}}(\gamma_{\text{th}})$. Here, $F_{\gamma_p^{(i,j)}}(\gamma)$ is the CDF of the instantaneous SINR of the PN in Scenario i-Case j. Specifically, $F_{\gamma_p^{(1,1)}}(\gamma)$, $F_{\gamma_p^{(2,2)}}(\gamma)$, and $F_{\gamma_p^{(3,1)}}(\gamma)$ are, respectively, given as follows:

Theorem 1 *The CDF of the instantaneous SINR $\gamma_p^{(1,1)}$ of the PN in Scenario 1-Case 1 can be expressed as*

$$\begin{aligned}
F_{\gamma_p^{(1,1)}}(\gamma) = 1 &- \sum_{p=0}^{m_3-1} \frac{\alpha_3^{p}\,(\beta_1+\beta_2)^{p}}{p!} \gamma^{p} \exp\left(-\alpha_3\,(\beta_1+\beta_2)\,\gamma\right) \\
&- \sum_{q=0}^{m_1-1} \frac{\alpha_1^{m_7} {\alpha_7}^{m_7}\,(\beta_1+\beta_2)^{m_7}}{q!\,\alpha_4^{m_7}} \frac{\Gamma\,(m_4+q)\,\Gamma\,(m_4+m_7)}{\Gamma\,(m_7)\,\Gamma\,(m_4)} \\
&\times \gamma^{m_7} U\left(m_4+m_7, m_7+1-q, \frac{\alpha_1\alpha_7\,(\beta_1+\beta_2)\,\gamma}{\alpha_4}\right) \\
&+ \sum_{p=0}^{m_3-1} \sum_{q=0}^{m_1-1} \frac{1}{p!} \frac{\alpha_1^{m_7} \alpha_3^{p} {\alpha_7}^{m_7}\,(\beta_1+\beta_2)^{m_7+p}}{q!\,\alpha_4^{m_7}} \\
&\times \frac{\Gamma(m_4+q)\,\Gamma\,(m_4+m_7)}{\Gamma(m_7)\Gamma(m_4)} \gamma^{m_7+p} \exp\left(-\alpha_3\,(\beta_1+\beta_2)\gamma\right) \\
&\times U\left(m_4+m_7, m_7+1-q, \frac{\alpha_1\alpha_7\gamma\,(\beta_1+\beta_2)}{\alpha_4}\right)
\end{aligned} \tag{57}$$

Proof See Appendix 1. □

Theorem 2 *The CDF of the instantaneous SINR $\gamma_p^{(2,2)}$ of the PN in Scenario 2-Case 2 can be derived as*

$$\begin{aligned}
F_{\gamma_p^{(2,2)}}(\gamma) = 1 &- \sum_{k=0}^{m_3-1} \sum_{n=0}^{k} \frac{C_n^k}{k!} \frac{\alpha_7^{m_7}\Gamma(m_7+n)}{\alpha_3^{m_7+n-k}\beta_2^{m_7+n-k}\beta_3^{m_7}\Gamma(m_7)} \\
&\times \frac{\gamma^k \exp(-\alpha_3\gamma\beta_2)}{[\gamma+\alpha_7\alpha_3^{-1}\beta_2^{-1}\beta_3^{-1}]^{m_7+n}} - \sum_{j=0}^{m_1-1}\sum_{l=0}^{j} \frac{1}{j!} \\
&\times \frac{C_l^j \alpha_2^{m_2}\alpha_4^{m_4}\Gamma(m_4+j)\Gamma(m_2+m_4+l)}{\beta_2^{m_4}\beta_3^{m_4+m_2}\alpha_1^{m_4}\Gamma(m_2)\Gamma(m_4)} \\
&\times \frac{U(m_2+m_4+l, m_2+l+1-j, \gamma\beta_2\alpha_1\alpha_2/(\gamma\beta_2\beta_3\alpha_1+\alpha_4))}{(\gamma+\alpha_7\alpha_3^{-1}\beta_2^{-1}\beta_3^{-1})^{m_4+m_2+l}} \\
&\times \gamma^{m_2+l} + \sum_{k=0}^{m_3-1}\sum_{n=0}^{k}\sum_{j=0}^{m_1-1}\sum_{l=0}^{j} \frac{C_n^k C_l^j}{k!\,j!} \\
&\times \frac{\alpha_2^{m_2}\alpha_4^{m_4}\alpha_7^{m_7}\Gamma(m_4+j)\Gamma(m_7+n)\Gamma(m_2+m_4+l)}{\beta_3^{m_2+m_4+m_7}\alpha_1^{m_4}\alpha_3^{m_7+n-k}\beta_2^{m_4+m_7+n-k}\Gamma(m_2)\Gamma(m_4)\Gamma(m_7)} \\
&\times \left[\sum_{t=1}^{m_7+n} \kappa_{nt} \frac{\gamma^{m_2+l+k}\exp(-\alpha_3\gamma\beta_2)}{\left[\gamma+\alpha_7\alpha_3^{-1}\beta_2^{-1}\beta_3^{-1}\right]^{t}}\right. \\
&\times U\left(m_2+m_4+l, m_2+l+1-j, \frac{\gamma\beta_2\alpha_1\alpha_2}{\gamma\beta_2\beta_3\alpha_1+\alpha_4}\right) \\
&+ \sum_{v=1}^{m_4+m_2+l} \chi_{lv} \frac{\gamma^{m_2+l+k}\exp(-\alpha_3\gamma\beta_2)}{\left[\gamma+\alpha_4\beta_2^{-1}\beta_3^{-1}\alpha_1^{-1}\right]^{k}} \\
&\left.\times U\left(m_2+m_4+l, m_2+l+1-j, \frac{\gamma\beta_2\alpha_1\alpha_2}{\gamma\beta_2\beta_3\alpha_1+\alpha_4}\right)\right]
\end{aligned} \tag{58}$$

where κ_{nt} and χ_{lv} are partial fraction coefficients calculated based on ([13], Eq. (3.326 .2)) *as*

$$\begin{aligned}
\kappa_{nt} = &\frac{1}{(m_7+n-t)!} \\
&\times \frac{d^{m_7+n-t}}{d\gamma^{m_7+n-t}} \left[\left(\gamma+\frac{\alpha_4}{\beta_2\beta_3\alpha_1}\right)^{-m_4-m_2-l}\right]\Big|_{\gamma=-\frac{\alpha_7}{\alpha_3\beta_2\beta_3}}
\end{aligned} \tag{59}$$

$$\begin{aligned}
\chi_{lv} = &\frac{1}{(m_4+m_2+l-v)!} \\
&\times \frac{d^{m_4+m_2+l-v}}{d\gamma^{m_4+m_2+l-v}} \left[\left(\gamma+\frac{\alpha_7}{\alpha_3\beta_2\beta_3}\right)^{-m_7-n}\right]\Big|_{\gamma=-\frac{\alpha_4}{\beta_2\beta_3\alpha_1}}
\end{aligned} \tag{60}$$

Proof See Appendix 2. □

Theorem 3 *The CDF of the instantaneous SINR $\gamma_p^{(3,1)}$ of the PN in Scenario 3-Case 1 can be derived as*

$$F_{\gamma_p^{(3,1)}}(\gamma) = \left[1 - \exp(-\alpha_3\beta_2\gamma)\sum_{i=0}^{m_3-1}\frac{\alpha_3^i\beta_2^i\gamma^i}{i!}\right] \times \left[1 - \sum_{j=0}^{m_1-1}\frac{2}{j!}\sum_{l=0}^{j}C_l^j\sum_{k=0}^{m_2-1}\frac{C_k^{m_2-1}}{\Gamma(m_2)}\alpha_1^{\frac{k+l+j+1}{2}} \times \alpha_2^{\frac{2m_2-k-l+j-1}{2}}\beta_2^{m_2+j}\gamma^{m_2+j}\exp(-(\alpha_1+\alpha_2)\beta_2\gamma) \times \mathcal{K}_{k+l-j+1}\left(2\sqrt{\alpha_1\alpha_2}\gamma\beta_2\right)\right] \quad (61)$$

Proof See Appendix 3. □

Substituting (9), (36), (48), (57), (58), and (61) into (56) and using $\gamma = \gamma_{\text{th}}$ as an argument, the outage probability of the PN can be straightforwardly derived.

3.2 Outage probability of the CCRN

Similarly, the outage probability of the SN can be obtained by applying (55) as

$$P_{s,\text{out}} = \frac{p_s^{(1,1)}P_{s,\text{out}}^{(1,1)} + p_s^{(1,2)}P_{s,\text{out}}^{(1,2)} + p_s^{(2,1)}P_{s,\text{out}}^{(2,1)} + p_s^{(2,2)}P_{s,\text{out}}^{(2,2)}}{p_s} \quad (62)$$

Here, $P_{s,\text{out}}^{(i,j)}$ is the outage probability of the SN in Scenario i-Case j, i.e., $P_{s,\text{out}}^{(i,j)} = F_{\gamma_s^{(i,j)}}(\gamma_{\text{th}})$ where $F_{\gamma_s^{(i,j)}}(\gamma)$ is the CDF of the instantaneous SINR $\gamma_s^{(i,j)}$.

First, we calculate the CDF of $\gamma_s^{(i,j)}$ in Scenario 1-Case 1. From (20), we have $\gamma_s^{(1,1)} = \max[\gamma_{1s}^{(1,1)}, \gamma_{2s}^{(1,1)}]$. Since X_7 appears in expression (18) of $\gamma_{1s}^{(1,1)}$ and (19) of $\gamma_{2s}^{(1,1)}$, we have $F_{\gamma_s^{(1,1)}}(\gamma) \neq F_{\gamma_{1s}^{(1,1)}}(\gamma)F_{\gamma_{2s}^{(1,1)}}(\gamma)$. However, due to the independence among the X_i, we have $F_{\gamma_s^{(1,1)}}(\gamma|X_7) = F_{\gamma_{1s}^{(1,1)}}(\gamma|X_7)F_{\gamma_{2s}^{(1,1)}}(\gamma|X_7)$. As a result, the unconditional CDF is obtained as

$$F_{\gamma_s^{(1,1)}}(\gamma) = \int_0^\infty F_{\gamma_{1s}^{(1,1)}}(\gamma|X_7)F_{\gamma_{2s}^{(1,1)}}(\gamma|X_7)f_{X_7}(x_7)dx_7 \quad (63)$$

From (18), $F_{\gamma_{1s}^{(1,1)}}(\gamma|X_7)$ is expressed as

$$F_{\gamma_{1s}^{(1,1)}}(\gamma|X_7) = \int_0^\infty F_{X_6}\left(\frac{\gamma x_7(x_8+\beta_2)}{\beta_1}\right)f_{X_8}(x_8)dx_8 \quad (64)$$

Substituting (1) and (2) into (64), then utilizing the Binomial theorem together with the help of ([13], Eq. (3.381.4)), we obtain

$$F_{\gamma_{1s}^{(1,1)}}(\gamma|X_7) = 1 - \sum_{i=0}^{m_6-1}\sum_{j=0}^{i}\frac{C_j^i}{i!}\frac{\alpha_8^{m_8}\beta_1{}^{m_8+j-i}\beta_2^{i-j}}{\alpha_6^{m_8+j-i}\gamma^{m_8+j-i}} \times \frac{\Gamma(m_8+j)}{\Gamma(m_8)}\frac{x_7^i\exp\left(-\alpha_6\beta_2\gamma x_7\beta_1^{-1}\right)}{\left(x_7+\alpha_8\beta_1\alpha_6^{-1}\gamma^{-1}\right)^{m_8+j}} \quad (65)$$

Further, $F_{\gamma_{2s}^{(1,1)}}(\gamma|X_7)$ can be approximated from (19) as

$$F_{\gamma_{2s}^{(1,1)}}(\gamma|X_7) = 1-[1-F_{\theta_1}(\gamma|X_7)]\,[1-F_{\theta_2}(\gamma)] \quad (66)$$

where $\theta_1 = \frac{\beta_1 X_4}{X_1 X_7}$ and $\theta_2 = \frac{\beta_1 X_5}{\beta_2 X_2}$. Then, $F_{\theta_1}(\gamma|X_7)$ and $F_{\theta_2}(\gamma)$ are given by

$$F_{\theta_1}(\gamma|X_7) = \int_0^\infty F_{X_4}\left(\frac{\gamma x_1 x_7}{\beta_1}\right)f_{X_1}(x_1)dx_1 \quad (67)$$

$$F_{\theta_2}(\gamma) = \int_0^\infty F_{X_5}\left(\frac{\gamma\beta_2 x_2}{\beta_1}\right)f_{X_2}(x_2)dx_2 \quad (68)$$

By substituting (1) and (2) into (67) and (68) together with the help of ([13], Eq. (3.381 .4)), we obtain expressions for $F_{\theta_1}(\gamma|X_7)$ and $F_{\theta_2}(\gamma)$. Then, substituting these outcomes into (66), an expression of $F_{\gamma_{2s}^{(1,1)}}(\gamma|X_7)$ can be derived as

$$F_{\gamma_{2s}^{(1,1)}}(\gamma|X_7) = 1 - \sum_{i=0}^{m_6-1}\frac{1}{i!}\sum_{j=0}^{i}C_j^i\frac{\alpha_8{}^{m_8}\beta_1{}^{m_8+j-i}\beta_2{}^{i-j}}{\alpha_6{}^{m_8+j-i}\gamma^{m_8+j-i}} \times \frac{\Gamma(m_8+j)}{\Gamma(m_8)}\frac{x_7 i\exp\left(-\alpha_6\beta_2\gamma x_7\beta_1^{-1}\right)}{\left(x_7+\alpha_8\beta_1\alpha_6^{-1}\gamma^{-1}\right)^{m_8+j}} \quad (69)$$

Now, we substitute (65), (69), and (1) into (63). Then, we apply ([13], Eq.(3.326.2)) to change the resulting integrals into computable forms. Finally, utilizing ([17], Eq. (2.3 .6.9)) to solve the integrals, we obtain

$$F_{\gamma_s^{(1,1)}}(\gamma) = 1 - \sum_{i=0}^{m_6-1} \sum_{j=0}^{i} \frac{C_j^i}{i!} \frac{\alpha_7^{m_7} \alpha_8^{m_7+i-j} \beta_1^{m_7}}{\alpha_6^{m_7} \gamma^{m_7} \beta_2^{j-i}} \times U\left(m_7+i, m_7+i+1-m_8-j, \beta_2\alpha_8 + \frac{\alpha_7\beta_1\alpha_8}{\alpha_6\gamma}\right) \times \frac{\Gamma(m_8+j)\Gamma(m_7+i)}{\Gamma(m_7)\Gamma(m_8)} - \sum_{p=0}^{m_4-1}\sum_{q=0}^{m_5-1}\frac{1}{p!\,q!} \times \frac{\Gamma(m_1+p)\Gamma(m_2+q)\Gamma(m_7+p)\alpha_1^{m_7}\alpha_2^{m_2}\alpha_5^{q}\alpha_7^{m_7}\beta_1^{m_7+m_2}\beta_2^{q}}{\Gamma(m_1)\Gamma(m_2)\Gamma(m_7)\alpha_4^{m_7}\gamma^{m_7-q}(\alpha_5\beta_2\gamma+\alpha_2\beta_1)^{m_2+q}} \times U\left(m_7+p, m_7+1-m_1, \frac{\alpha_1\alpha_7\beta_1}{\alpha_4\gamma}\right) + \sum_{p=0}^{m_4-1}\sum_{q=0}^{m_5-1}\sum_{i=0}^{m_6-1}\sum_{j=0}^{i} \times \frac{C_j^i \beta_1^{m_1+m_2+m_8+j-i}\beta_2^{q+i-j}\alpha_1^{m_1}\alpha_2^{m_2}}{p!\,q!\,i!\,\alpha_4^{m_1}\alpha_6^{m_8+j-i}} \times \frac{\alpha_5^{q}\alpha_7^{m_7}\alpha_8^{m_8}\Gamma(m_1+p)\Gamma(m_2+q)\Gamma(m_7+p+i)\Gamma(m_8+j)}{\Gamma(m_1)\Gamma(m_2)\Gamma(m_7)\Gamma(m_8)} \times \frac{1}{\gamma^{m_1+m_8+j-i-q}(\alpha_5\beta_2\gamma+\alpha_2\beta_1)^{m_2+q}} \times \left[\sum_{l=1}^{m_8+j}\kappa_{jl}\left(\frac{\alpha_8\beta_1}{\alpha_6\gamma}\right)^{m_7+p+i-l} U\left(m_7+p+i, m_7+p+i+1-l,\ \alpha_8\beta_2+\frac{\alpha_7\alpha_8\beta_1}{\alpha_6\gamma}\right) + \sum_{k=1}^{m_1+p}\chi_{pk}\left(\frac{\alpha_1\beta_1}{\alpha_4\gamma}\right)^{m_7+p+i-k} \times U\left(m_7+p+i, m_7+p+i+1-k, \frac{\alpha_1\alpha_6\beta_2\gamma+\alpha_1\alpha_7\beta_1}{\alpha_4\gamma}\right)\right] \tag{70}$$

where κ_{jl} and χ_{pk} are partial fraction coefficients, respectively, defined as

$$\kappa_{jl} = \frac{1}{(m_8+j-l)!} \times \left.\frac{d^{m_8+j-l}\left[x+\alpha_1\beta_1\alpha_4^{-1}\gamma^{-1}\right]^{-m_1-p}}{dx^{m_8+j-l}}\right|_{x=-\alpha_8\beta_1\alpha_6^{-1}\gamma^{-1}} \tag{71}$$

$$\chi_{pk} = \frac{1}{(m_1+p-k)!} \times \left.\frac{d^{m_1+p-k}\left[x+\alpha_8\beta_1\alpha_6^{-1}\gamma^{-1}\right]^{-m_8-j}}{dx^{m_1+p-k}}\right|_{x=-\alpha_1\beta_1\alpha_4^{-1}\gamma^{-1}} \tag{72}$$

Using the same approach of calculating $F_{\gamma_s^{(1,1)}}(\gamma)$ in Scenario 1-Case 1, $F_{\gamma_s^{(1,2)}}(\gamma)$ in Scenario 1-Case 2 and $F_{\gamma_s^{(2,2)}}(\gamma)$ in Scenario 2-Case 2 are attained as

$$F_{\gamma_s^{(1,2)}}(\gamma) = 1 - \sum_{i=0}^{m_6-1}\frac{\beta_1^{m_7}\alpha_7^{m_7}\Gamma(m_7+i)}{i!\,\alpha_6^{m_7}\beta_2^{m_7}\Gamma(m_7)}\frac{\gamma^i}{\left(\gamma+\alpha_7\beta_1\alpha_6^{-1}\beta_2^{-1}\right)^{m_7+i}} - \sum_{j=0}^{m_4-1}\sum_{k=0}^{m_5-1}\frac{\beta_1^{m_2+m_7}\alpha_2^{m_2}}{j!\,k!\,\beta_2^{m_2+m_7}}\frac{\alpha_7^{m_7}\Gamma(m_7+j)\Gamma(m_2+k)}{\alpha_4^{m_7}\alpha_5^{m_2}\Gamma(m_2)\Gamma(m_7)} \times \left[\sum_{l=1}^{m_7+j}\frac{\kappa_{jl}\gamma^{j+k}}{\left(\gamma+\beta_1\alpha_7\beta_2^{-1}\alpha_4^{-1}\right)^l} + \sum_{m=1}^{m_2+k}\frac{\chi_{km}\gamma^{j+k}}{\left(\gamma+\alpha_2\beta_1\alpha_5^{-1}\beta_2^{-1}\right)^k}\right] + \sum_{i=0}^{m_6-1}\sum_{j=0}^{m_4-1}\sum_{k=0}^{m_5-1}\frac{\beta_1^{m_2+m_7}}{i!\,j!\,k!}\frac{\alpha_2^{m_2}\alpha_4^{j}\alpha_6^{i}\alpha_7^{m_7}}{\beta_2^{m_2+m_7}\alpha_5^{m_2}(\alpha_4+\alpha_6)^{m_7+i+j}} \times \frac{\Gamma(m_2+k)\Gamma(m_7+i+j)}{\Gamma(m_2)\Gamma(m_7)}\left[\sum_{n=1}^{m_7+k}\frac{\xi_{kn}\gamma^{i+j+k}}{\left(\gamma+\alpha_2\beta_1\alpha_5^{-1}\beta_2^{-1}\right)^n} + \sum_{t=1}^{m_7+i+j}\frac{\theta_{ijt}\gamma^{i+j+k}}{[\gamma+\alpha_7\beta_1(\alpha_4\beta_2+\alpha_6\beta_2)^{-1}]^t}\right] \tag{73}$$

$$F_{\gamma_s^{(2,2)}}(\gamma) = 1 - \sum_{i=0}^{m_6-1}\sum_{j=0}^{i}\frac{C_j^i}{i!}\frac{\beta_2^{m_8}\beta_3^{m_8+j-i}\alpha_8^{m_8}}{\alpha_6^{m_8+j-i}}\frac{\Gamma(m_8+j)\gamma^i\exp(-\alpha_6\gamma/\beta_3)}{\Gamma(m_8)(\gamma+\beta_2\beta_3\alpha_8/\alpha_6)^{m_8+j}} - \sum_{p=0}^{m_4-1}\sum_{q=0}^{m_5-1}\frac{\alpha_1^{m_1}\alpha_5^{q}\beta_2^{m_1}}{p!\,q!\,\alpha_4^{m_1}}\frac{\beta_3^{m_1-q}\Gamma(m_1+p)\gamma^{p+q}\exp(-\alpha_5\gamma/\beta_3)}{\Gamma(m_1)(\gamma+\alpha_1\beta_2\beta_3/\alpha_4)^{m_1+p}} + \sum_{i=0}^{m_6-1}\sum_{j=0}^{i}\sum_{p=0}^{m_4-1}\sum_{q=0}^{m_5-1}\frac{C_j^i\alpha_1^{m_1}\alpha_5^{q}\alpha_8^{m_8}\beta_2^{m_1+m_8}\beta_3^{m_1+m_8+j-i-q}}{i!\,p!\,q!\,\alpha_4^{m_1}\alpha_6^{m_8+j-i}} \times \frac{\Gamma(m_1+p)\Gamma(m_8+j)}{\Gamma(m_1)\Gamma(m_8)}\left[\sum_{l=1}^{m_8+j}\frac{\mu_{lj}\gamma^{i+p+q}}{(\gamma+\beta_2\beta_3\alpha_8/\alpha_6)^l} + \sum_{k=1}^{m_1+p}\frac{\eta_{ki}\gamma^{i+p+q}}{(\gamma+\alpha_1\beta_2\beta_3/\alpha_4)^k}\right]\exp\left(-\frac{(\alpha_5+\alpha_6)\gamma}{\beta_3}\right) \tag{74}$$

where ξ_{kn}, θ_{ijt}, μ_{lj}, and η_{ki} are partial fraction coefficients, respectively, defined as

$$\xi_{kn} = \frac{1}{(m_2+k-n)!} \times \left.\frac{d^{m_7+k-n}\left[\gamma+\alpha_7\beta_1/(\alpha_4\beta_2+\alpha_6\beta_2)\right]^{-m_7-i-j}}{d\gamma^{m_7+k-n}}\right|_{\gamma=-\alpha_2\beta_1\alpha_5^{-1}\beta_2^{-1}} \tag{75}$$

$$\theta_{ijt} = \frac{1}{(m_7+i+j-t)!} \times \left.\frac{d^{m_7+i+j-t}\left[\gamma+\alpha_2\beta_1\alpha_5^{-1}\beta_2^{-1}\right]^{-m_2-k}}{d\gamma^{m_7+i+j-t}}\right|_{\gamma=-\alpha_7\beta_1(\alpha_4\beta_2+\alpha_6\beta_2)^{-1}} \tag{76}$$

$$
\begin{aligned}
\mu_{lj} &= \frac{1}{(m_8+j-l)!} \\
&\quad \times \left. \frac{d^{m_8+j-l}\left[(\gamma+\alpha_1\beta_2\beta_3/\alpha_4)^{-m_1-p}\right]}{d\gamma^{m_8+j-l}} \right|_{\gamma=-\beta_2\beta_3\alpha_8/\alpha_6} \\
\eta_{ki} &= \frac{1}{(m_1+p-k)!} \\
&\quad \times \left. \frac{d^{m_1+p-k}\left[(\gamma+\beta_2\beta_3\alpha_8/\alpha_6)^{-m_8-j}\right]}{d\gamma^{m_1+p-k}} \right|_{\gamma=-\alpha_1\beta_2\beta_3/\alpha_4}
\end{aligned}
\tag{77}
$$

Utilizing the same approach of calculating $F_{\gamma_p^{(3,1)}}(\gamma)$ in Scenario 3 of the PN, the CDF of $\gamma_s^{(2,1)}$ in Scenario 2-Case 1 of the SN can be expressed as

$$
\begin{aligned}
F_{\gamma_s^{(2,1)}}(\gamma) &= \left[1-\exp\left(-\frac{\alpha_6\gamma}{\beta_3}\right)\sum_{l=0}^{m_6-1}\frac{1}{l!}\frac{\alpha_6^l\gamma^l}{\beta_3^l}\right] \\
&\quad \times \left[1-\sum_{k=0}^{m_4-1}\frac{2}{k!}\sum_{t=0}^{k}\sum_{h=0}^{m_5-1}\frac{C_t^k C_h^{m_5-1}}{\Gamma(m_5)}\frac{\alpha_4^{(h+t+k+1)/2}}{\beta_3^{m_5+k}}\right. \\
&\quad \times \alpha_5^{\frac{2m_5-h-t+k-1}{2}}\gamma^{m_5+k}\exp\left(-\frac{(\alpha_4+\alpha_5)\gamma}{\beta_3}\right) \\
&\quad \left.\times\, \mathcal{K}_{h+t-k+1}\left(\frac{2\gamma\sqrt{\alpha_4\alpha_5}}{\beta_3}\right)\right]
\end{aligned}
\tag{78}
$$

Finally, substituting (9), (21), (29), (36), (70), (73), (74), and (78) into (62) and using $\gamma=\gamma_{th}$ as an argument, the outage probability for the CCRN is obtained.

4 Outage capacity analysis

The outage capacity C_ϵ corresponding to outage probability ϵ% can be approximated as [18]

$$
C_\epsilon = E\{C\}+\sqrt{2\left(E\{C^2\}-E^2\{C\}\right)}\operatorname{erfc}^{-1}\left[2-\epsilon/50\right]
\tag{79}
$$

where $\operatorname{erfc}^{-1}[\cdot]$ is the inverse complementary error function. Furthermore, $E\{C\}$ and $E\{C^2\}$ are the first and second moment of the channel capacity, respectively. Based on the Shannon capacity theorem, the rth moment of the channel capacity is given by

$$
\begin{aligned}
E\left\{C^r\right\} &= \int_0^\infty\left(\frac{\ln(1+\gamma)}{2\ln 2}\right)^r f_\gamma(\gamma)d\gamma \\
&= \frac{1}{2(\ln 2)^r}\int_0^\infty\frac{[\ln(1+\gamma)]^{r-1}\left[1-F_{\gamma_p}(\gamma)\right]}{1+\gamma}d\gamma
\end{aligned}
\tag{80}
$$

4.1 Outage capacity of the PN

Outage capacity $C_{p,\epsilon}$ in (bits/s/Hz) of the PN, i.e., the largest rate to guarantee that the outage probability is less than ϵ%, is derived from (55) as

$$
C_{p,\epsilon} = \frac{p_p^{(1,1)}C_{p,\epsilon}^{(1,1)}+p_p^{(2,2)}C_{p,\epsilon}^{(2,2)}+p_p^{(3,1)}C_{p,\epsilon}^{(3,1)}}{p_p}
\tag{81}
$$

where $C_{p,\epsilon}^{(i,j)}$ is the outage capacity of the PN in Scenario i-Case j. In order to obtain $C_{p,\epsilon}^{(i,j)}$, we need to calculate the first and second moment of the channel capacity. Substituting (57) into (80), the rth moment of the channel capacity of the PN in Scenario 1-Case 1 is given by

$$
\begin{aligned}
E\left\{C_p^{(1,1)^r}\right\} &= \frac{1}{2(\ln 2)^r}\sum_{p=0}^{m_3-1}\frac{\alpha_3^p(\beta_1+\beta_2)^p}{p!} \\
&\quad \times T\left(\alpha_3(\beta_1+\beta_2),p,0,0,0,0,0,0,0,1,r-1,1\right) \\
&\quad + \frac{1}{2(\ln 2)^r}\sum_{q=0}^{m_1-1}\frac{\alpha_1^{m_7}\alpha_7{}^{m_7}(\beta_1+\beta_2)^{m_7}}{q!\,\alpha_4^{m_7}} \\
&\quad \times \frac{\Gamma(m_4+q)\Gamma(m_4+m_7)}{\Gamma(m_7)\Gamma(m_4)}T(0,m_7,0,0,m_4 \\
&\quad + m_7,m_7+1-q,\alpha_1\alpha_7(\beta_1+\beta_2)),0,0,\alpha_4,r-1,1) \\
&\quad - \frac{1}{2(\ln 2)^r}\sum_{p=0}^{m_3-1}\sum_{q=0}^{m_1-1}\frac{\alpha_1^{m_7}\alpha_3^p\alpha_7{}^{m_7}(\beta_1+\beta_2)^{m_7+p}}{p!\,q!\,\alpha_4^{m_7}} \\
&\quad \times \frac{\Gamma(m_4+q)\Gamma(m_4+m_7)}{\Gamma(m_7)\Gamma(m_4)}T(\alpha_3(\beta_1+\beta_2),m_7+p,0,0,m_4 \\
&\quad + m_7,m_7+1-q,\alpha_1\alpha_7(\beta_1+\beta_2)),0,0,\alpha_4,r-1,1)
\end{aligned}
\tag{82}
$$

where $T(a,b,c,d,e,f,g,h,i,j,k,l) = \int_0^\infty\frac{e^{-\gamma a}\gamma^b}{(\gamma+c)^d}\times U\left(e,f,\frac{g\gamma+h}{i\gamma+j}\right)\frac{(\ln(1+\gamma))^k}{(1+\gamma)^l}d\gamma$.

In the same way, the rth moment of the channel capacity of the PN in Scenario 2-Case 2 can be obtained by substituting (58) into (80) as

$$
\begin{aligned}
&E\left\{C_p^{(2,2)^r}\right\} \\
&= \frac{1}{2(\ln 2)^r}\left\{\sum_{k=0}^{m_3-1}\sum_{n=0}^{k}\frac{C_n^k\alpha_7^{m_7}\Gamma(m_7+n)T\left(\alpha_3\beta_2,k,\frac{\alpha_7}{\alpha_3\beta_2\beta_3},m_7+n,0,0,0,1,0,1,r-1,1\right)}{k!\,\alpha_3{}^{m_7+n-k}\beta_2{}^{m_7+n-k}\beta_3{}^{m_7}\Gamma(m_7)}\right. \\
&\quad + \sum_{j=0}^{m_1-1}\sum_{l=0}^{j}T\left(0,m_2+l,\frac{\alpha_3^{-1}\alpha_7}{\beta_2\beta_3},m_4+m_2+l,m_2+m_4+l,m_2+l+1-j,\beta_2\alpha_1\alpha_2,0,\right. \\
&\quad \left.\beta_2\beta_3\alpha_1,\alpha_4,r-1,1\right)\frac{C_l^j}{j!}\frac{\alpha_2^{m_2}\alpha_4^{m_4}}{\beta_2^{m_4}\beta_3^{m_4+m_2}\alpha_1^{m_4}\Gamma(m_2)\Gamma(m_4)}\Gamma(m_4+j)\Gamma(m_2+m_4+l) \\
&\quad - \sum_{k=0}^{m_3-1}\sum_{n=0}^{k}\sum_{j=0}^{m_1-1}\sum_{l=0}^{j}\frac{C_n^kC_l^j}{j!\,k!}\frac{1}{\Gamma(m_2)}\Gamma(m_4+j)\Gamma(m_7+n)\Gamma(m_2+m_4+l) \\
&\quad \times \frac{\alpha_1^{-m_4}\alpha_2^{m_2}\alpha_4^{m_4}\alpha_7^{m_7}}{\Gamma(m_4)\Gamma(m_7)\beta_3^{m_2+m_4+m_7}\alpha_3^{m_7+n-k}\beta_2^{m_4+m_7+n-k}}\left[\sum_{t=1}^{m_7+n}\kappa_{nt}T\left(\alpha_3\beta_2,m_2+l+k,\right.\right. \\
&\quad \left.\frac{\alpha_3^{-1}\alpha_7}{\beta_2\beta_3},t,m_2+m_4+l,m_2+l+1-j,\beta_2\alpha_1\alpha_2,0,\beta_2\beta_3\alpha_1,\alpha_4,r-1,1\right)+\sum_{v=1}^{m_4+m_2+l}\chi_{lv} \\
&\quad \times T\left(\alpha_3\beta_2,m_2+l+k,\frac{\alpha_4\alpha_1^{-1}}{\beta_2\beta_3},k,m_2+m_4+l,m_2+l+1-j,\beta_2\alpha_1\alpha_2,0,\beta_2\beta_3\alpha_1,\alpha_4,r\right. \\
&\quad \left.\left.\left.-\ 1,1\right)\right]\right\}
\end{aligned}
\tag{83}
$$

Similarly, the rth moment of the channel capacity of the PN in Scenario 3 can be obtained by substituting (61) into (80) as

$$E\left\{C_p^{(3,1)^r}\right\} = \sum_{i=0}^{m_3-1} \frac{\alpha_3^i \beta_2^i \Upsilon(i, r-1, \alpha_3\beta_2, 0, 0, 0)}{i!\, 2(\ln 2)^r} + \sum_{j=0}^{m_1-1}\sum_{l=0}^{j}\sum_{k=0}^{m_2-1} \times \frac{C_l^j C_k^{m_2-1}}{2j!\,(\ln 2)^r} \Upsilon(m_2+j, r-1, (\alpha_1+\alpha_2)\beta_2, k+l-j+1, 1, 2\beta_2\sqrt{\alpha_1\alpha_2}) \frac{\alpha_1^{\frac{k+l+j+1}{2}} \alpha_2^{\frac{2m_2-k-l+j-1}{2}} \beta_2^{m_2+j}}{\Gamma(m_2)} - \sum_{j=0}^{m_1-1}\sum_{l=0}^{j}\sum_{k=0}^{m_2-1}\sum_{i=0}^{m_3-1} \frac{C_l^j}{j!\,i!} \frac{C_k^{m_2-1}}{2(\ln 2)^r} \frac{\alpha_1^{\frac{k+l+j+1}{2}}}{\Gamma(m_2)} \times \alpha_2^{(2m_2-k-l+j-1)/2} \alpha_3^i \beta_2^{m_2+i+j} \Upsilon\left(m_2+j+i, r-1, (\alpha_1+\alpha_2+\alpha_3)\beta_2, k+l-j+1, 1, 2\beta_2\sqrt{\alpha_1\alpha_2}\right) \tag{84}$$

where $\Upsilon(a,b,c,d,e,f) = \int_0^\infty \frac{\gamma^a \ln^b(1+\gamma)\exp(-c\gamma)}{1+\gamma} \mathcal{K}_d{}^e(f\gamma)d\gamma$.

Substituting (82), (83), and (84) into (79), we obtain the outage capacity $C_{p,\epsilon}^{(i,j)}$ of the PN in Scenario i-Case j. Then, substituting these outcomes together with (9), (36), and (48) into (81) allows us to obtain the outage capacity for the PN.

4.2 Outage capacity of the CCRN

Similarly, outage capacity, $C_{s,\epsilon}$, in (bits/s/Hz) of the SN is derived from (55) as

$$C_{s,\epsilon} = \frac{p_s^{(1,1)} C_{s,\epsilon}^{(1,1)} + p_s^{(1,2)} C_{s,\epsilon}^{(1,2)} + p_s^{(2,1)} C_{s,\epsilon}^{(2,1)} + p_s^{(2,2)} C_{s,\epsilon}^{(2,2)}}{p_s} \tag{85}$$

where $C_{s,\epsilon}^{(i,j)}$ is the outage capacity in Scenario i-Case j of the SN. Substituting (70), (73), (74), and (78) into (80), the rth moment of the channel capacity of the CCRN in Scenario i-Case j are obtained. In particular, the rth moments of the channel capacity of the CCRN in Scenario 1-Case 1 is given by

$$E\left\{C_s^{(1,1)^r}\right\} = \sum_{i=0}^{m_6-1}\sum_{j=0}^{i} \frac{C_j^i \alpha_7^{m_7} \alpha_8^{m_7+i-j} \beta_1^{m_7} \Gamma(m_8+j)\Gamma(m_7+i)}{2(\ln 2)^r i!\, \alpha_6^{m_7} \beta_2^{j-i} \Gamma(m_8)\Gamma(m_7)} \times T\left(0, -m_7, 0, 0, m_7+i, m_7+i+1-m_8 - j, \alpha_8\beta_2, \alpha_7\alpha_8\beta_1/\alpha_6, 1, 0, r-1, 1\right) + \sum_{p=0}^{m_4-1}\sum_{q=0}^{m_5-1} \frac{\alpha_1{}^{m_7}\alpha_2{}^{m_2}\alpha_7{}^{m_7}\beta_1{}^{m_7+m_2}\Gamma(m_2+q)}{2(\ln 2)^r p!\, q!\, \alpha_4{}^{m_7}\alpha_5{}^{m_2}\beta_2{}^{m_2}} \times \frac{\Gamma(m_1+p)\Gamma(m_7+p)}{\Gamma(m_1)\Gamma(m_2)\Gamma(m_7)} T\left(0, q-m_7, \frac{\alpha_2\beta_1}{\alpha_5\beta_2}, m_2 + q, m_7+p, m_7+1-m_1, 0, \frac{\alpha_1\alpha_7\beta_1}{\alpha_4}, 1, 0, r-1, 1\right) - \sum_{p=0}^{m_4-1}\sum_{q=0}^{m_5-1}\sum_{i=0}^{m_6-1}\sum_{j=0}^{i} \frac{C_j^i \alpha_2^{m_2}\alpha_7^{m_7}\alpha_8^{m_8}\beta_1^{m_1+m_2+m_8+j-i}}{2(\ln 2)^r p!\, q!\, i!\, \alpha_1^{-m_1}\alpha_4^{m_1}\alpha_6^{m_8+j-i}} \times \frac{\Gamma(m_2+q)\Gamma(m_1+p)\Gamma(m_8+j)\Gamma(m_7+p+i)}{\beta_2^{m_2-i+j}\alpha_5^{m_2}\Gamma(m_1)\Gamma(m_2)\Gamma(m_7)\Gamma(m_8)} \times \left[\sum_{l=1}^{m_8+j} \kappa_{lj} \left(\frac{\alpha_8\beta_1}{\alpha_6}\right)^{m_7+p+i-l} T\left(0, q+l-m_1-m_7-m_8-j-p, \frac{\alpha_2\beta_1}{\alpha_5\beta_2}, m_2+q, m_7+p+i, m_7+p+i+1-l, \alpha_8\beta_2, \frac{\alpha_7\alpha_8\beta_1}{\alpha_6}, 1, 0, r-1, 1\right) + \sum_{k=1}^{m_1+p} \chi_{kp} \left(\frac{\alpha_1\beta_1}{\alpha_4}\right)^{m_7+p+i-k} T\left(0, q+k-m_1-m_7-m_8-j-p, \frac{\alpha_2\beta_1}{\alpha_5\beta_2}, m_2+q, m_7+p+i, m_7+p+i+1-k, \frac{\alpha_1\alpha_6}{\alpha_4\beta_2^{-1}}, \frac{\alpha_1\alpha_7}{\alpha_4\beta_1^{-1}}, 1, 0, r-1, 1\right)\right] \tag{86}$$

Then, the rth moment of the channel capacity of the CCRN in Scenario 1-Case 2 is given by

$$E\left\{C_s^{(1,2)^r}\right\} = \sum_{i=0}^{m_6-1} \frac{\beta_1^{m_7}\beta_2^{-m_7}\alpha_7^{m_7}\Gamma(m_7+i)}{2(\ln 2)^r i!\, \alpha_6{}^{m_7}\Gamma(m_7)} \times T\left(0, i, \frac{\alpha_7\beta_1}{\alpha_6\beta_2}, m_7+i, 0, 0, 0, 1, 0, 1, r-1, 1\right) + \sum_{j=0}^{m_4-1}\sum_{k=0}^{m_5-1} \frac{\beta_1^{m_2+m_7}}{2(\ln 2)^r} \frac{\alpha_2^{m_2}\alpha_7^{m_7}\Gamma(m_2+k)\Gamma(m_7+j)}{j!\, k!\, \beta_2^{m_2+m_7}\alpha_4^{m_7}\alpha_5^{m_2}\Gamma(m_2)\Gamma(m_7)} \times \left[\sum_{l=1}^{m_7+j} \kappa_{jl} T\left(0, j+k, \frac{\beta_1\alpha_7}{\beta_2\alpha_4}, l, 0, 0, 0, 1, 0, 1, r-1, 1\right) + \sum_{m=1}^{m_2+k} \chi_{km}\, T\left(0, j+k, \frac{\alpha_2\beta_1}{\alpha_5\beta_2}, k, 0, 0, 0, 1, 0, 1, 1, 1\right)\right] - \sum_{k=0}^{m_5-1} \frac{\beta_1^{m_2+m_7}\alpha_2^{m_2}\alpha_4^{j}\alpha_5^{-m_2}\alpha_6^{i}\alpha_7^{m_7}\Gamma(m_2+k)\Gamma(m_7+i+j)}{2(\ln 2)^r i!\, j!\, k!\, \beta_2^{m_2+m_7}(\alpha_4+\alpha_6)^{m_7+i+j}\Gamma(m_2)\Gamma(m_7)} \times \left[\sum_{n=1}^{m_7+k} \xi_{kn} T\left(0, i+j+k, \frac{\alpha_2\beta_1}{\alpha_5\beta_2}, n, 0, 0, 0, 1, 0, 1, 1, 1\right) + \sum_{t=1}^{m_7+i+j} \theta_{ijt} T\left(0, j+k, \frac{\alpha_7\beta_1\beta_2^{-1}}{\alpha_4+\alpha_6}, t, 0, 0, 0, 1, 0, 1, r-1, 1\right)\right] \tag{87}$$

Further, the rth moment of the channel capacity of the CCRN in Scenario 2-Case 1 is obtained as

$$E\left\{C_s^{(2,1)^r}\right\} = \sum_{l=0}^{m_6-1} \frac{\alpha_6^l \Upsilon\left(l, r-1, \frac{\alpha_6}{\beta_3}, 0, 0, 0\right)}{2(\ln 2)^r l!\, \beta_3^l} + \sum_{k=0}^{m_4-1}\sum_{t=0}^{k} \frac{C_t^k}{k!} \times \sum_{h=0}^{m_5-1} \frac{C_h^{m_5-1}}{\Gamma(m_5)} \frac{\alpha_4^{(h+t+k+1)/2}\alpha_5^{(2m_5-h-t+k-1)/2}}{(\ln 2)^r \beta_3^{m_5+k}}$$

$$\times \Upsilon\left(m_5+k, r-1, \frac{(\alpha_4+\alpha_5)}{\beta_3}, h+t-k+1, 1, \frac{2\sqrt{\alpha_4\alpha_5}}{\beta_3}\right) - \sum_{k=0}^{m_4-1}\sum_{t=0}^{k}\sum_{h=0}^{m_5-1}\frac{C_t^k}{k!}\frac{C_h^{m_5-1}\alpha_4^{(h+t+k+1)/2}}{\Gamma(m_5)} \times \frac{\alpha_5^{(2m_5-h-t+k-1)/2}}{(\ln 2)^r\beta_3^{m_5+k}}\sum_{l=0}^{m_6-1}\frac{1}{l!}\frac{\alpha_6^l}{\beta_3^l} \Upsilon\left(m_5+k+l, r-1, \frac{(\alpha_4+\alpha_5+\alpha_6)}{\beta_3}, h+t-k+1, 1, \frac{2\sqrt{\alpha_4\alpha_5}}{\beta_3}\right) \tag{88}$$

Finally, the rth moment of the channel capacity of the CCRN in Scenario 2-Case 2 is derived as

$$E\left\{C_s^{(2,2)^r}\right\} = \sum_{i=0}^{m_6-1}\sum_{j=0}^{i}\frac{C_j^i\beta_2^{m_8}\beta_3^{m_8+j-i}\alpha_8^{m_8}}{2(\ln 2)^r i!\,\alpha_6^{m_8+j-i}}\frac{\Gamma(m_8+j)}{\Gamma(m_8)} \times T\left(\frac{\alpha_6}{\beta_3}, i, \frac{\beta_2\beta_3\alpha_8}{\alpha_6}, m_8+j, 0,0,0,1,0,1,r-1,1\right) + \sum_{p=0}^{m_4-1}\sum_{q=0}^{m_5-1}\frac{\alpha_5^q\beta_2^{m_1}\beta_3{}^{m_1-q}\Gamma(m_1+p)}{2(\ln 2)^r p!\,q!\,\alpha_1^{-m_1}\alpha_4^{m_1}\Gamma(m_1)} \times T\left(\frac{\alpha_5}{\beta_3}, p+q, \frac{\beta_2\beta_3}{\alpha_1^{-1}\alpha_4}, m_1+p, 0,0,0,1,0,1,r-1,1\right) - \sum_{i=0}^{m_6-1}\sum_{j=0}^{i}\sum_{p=0}^{m_4-1}\sum_{q=0}^{m_5-1}\frac{C_j^i\alpha_5^q\alpha_8^{m_8}\beta_2^{m_1+m_8}\beta_3^{m_1+m_8+j-i-q}}{2(\ln 2)^r i!\,p!\,q!\,\alpha_1^{-m_1}\alpha_4^{m_1}\alpha_6^{m_8+j-i}} \times \frac{\Gamma(m_1+p)\Gamma(m_8+j)}{\Gamma(m_1)\Gamma(m_8)}\left[\sum_{l=1}^{m_8+j}\mu_{lj}T\left(\frac{\alpha_5+\alpha_6}{\beta_3}, i+p+q, \frac{\beta_2\beta_3}{\alpha_6\alpha_8^{-1}}, l, 0,0,0,1,0,1,r-1,1\right) + \sum_{k=1}^{m_1+p}\eta_{ki} \times T\left(\frac{\alpha_5+\alpha_6}{\beta_3}, i+p+q, \frac{\alpha_1\beta_2\beta_3}{\alpha_4}, k, 0,0,0,1,0,1,r-1,1\right)\right] \tag{89}$$

By substituting (86), (87), (88), and (89) into (79), we obtain the outage capacity $C_{s,\epsilon}^{(i,j)}$. Then, substituting these outcomes together with (9), (21), (29), and (36) into (85), the outage capacity of the SN is obtained.

5 Symbol error rate analysis

According to [19], with modulation parameters α and β, the SER is expressed in terms of the CDF of the instantaneous SINR as

$$P_e = \frac{\alpha\sqrt{\beta}}{2\sqrt{\pi}}\int_0^\infty F_\gamma(\gamma)\gamma^{-\frac{1}{2}}e^{-\beta\gamma}d\gamma \tag{90}$$

5.1 Symbol error rate of the PN

Based on (55), the SER for the PN can be obtained as

$$P_{p,e} = \frac{p_p^{(1,1)}P_{p,e}^{(1,1)} + p_p^{(2,2)}P_{p,e}^{(2,2)} + p_p^{(3,1)}P_{p,e}^{(3,1)}}{p_p} \tag{91}$$

where $P_{p,e}^{(i,j)}$ is the SER of the PN in Scenario i-Case j. Substituting (57) into (90) and utilizing ([13], Eq. (3.381.4)), we obtain $P_{p,e}^{(1,1)}$ of the PN in Scenario 1-Case 1 as

$$P_{p,e}{}^{(1,1)} = \frac{\alpha}{2} - \frac{\alpha\sqrt{\beta}}{2\sqrt{\pi}}\sum_{p=0}^{m_3-1}\frac{1}{p!}\frac{\alpha_3^p(\beta_1+\beta_2)^p\Gamma\left(p+\frac{1}{2}\right)}{((\beta+\alpha_3(\beta_1+\beta_2)))^{p+\frac{1}{2}}} - \frac{\alpha\sqrt{\beta}}{2\sqrt{\pi}}\sum_{q=0}^{m_1-1}\frac{1}{q!}\frac{\alpha_1^{m_7}\alpha_7{}^{m_7}(\beta_1+\beta_2)^{m_7}}{\alpha_4^{m_7}} \times \frac{\Gamma(m_4+q)\Gamma(m_4+m_7)}{\Gamma(m_7)\Gamma(m_4)}T\left(\beta, m_7-\frac{1}{2}, 0, 0, m_4 + m_7, m_7+1-q, \alpha_1\alpha_7(\beta_1+\beta_2), 0, 0, \alpha_4, 0, 0\right) + \frac{\alpha\sqrt{\beta}}{2\sqrt{\pi}}\sum_{p=0}^{m_3-1}\sum_{q=0}^{m_1-1}\frac{\alpha_1^{m_7}\alpha_3^p}{p!\,q!}\frac{\alpha_7{}^{m_7}(\beta_1+\beta_2)^{m_7+p}}{\alpha_4^{m_7}} \times \frac{\Gamma(m_4+q)\Gamma(m_4+m_7)}{\Gamma(m_7)\Gamma(m_4)}T(\beta+\alpha_3(\beta_1+\beta_2), m_7+p-\frac{1}{2}, 0, 0, m_4+m_7, m_7+1-q, \alpha_1\alpha_7 \times(\beta_1+\beta_2), 0, 0, \alpha_4, 0, 0) \tag{92}$$

An expression for the SER, $P_{p,e}^{(2,2)}$ can be derived by first substituting (58) into (90). Then, we apply ([17], Eq. (2.3.8.1)) to solve the resulting integrals and finally an expression for $P_{p,e}^{(2,2)}$ of the PN in Scenario 2-Case 2 is given by

$$P_{p,e}^{(2,2)} = \frac{\alpha}{2} - \frac{\alpha\sqrt{\beta}}{2\sqrt{\pi}}\left\{\sum_{k=0}^{m_3-1}\sum_{n=0}^{k}\frac{C_n^k\Gamma(m_7+n)\Gamma(k+1/2)}{k!\,\alpha_3^{\frac{1}{2}}\beta_2^{\frac{1}{2}}\alpha_7^{n-k-\frac{1}{2}}\Gamma(m_7)} \times \beta_3^{n-k-\frac{1}{2}}U\left(k+\frac{1}{2}, k-m_7-n+\frac{3}{2}, \frac{\beta+\alpha_3\beta_2}{\alpha_3\beta_2\beta_3\alpha_7^{-1}}\right) + \sum_{j=0}^{m_1-1}\sum_{l=0}^{j}T\left(\beta, m_2+l-\frac{1}{2}, \frac{\alpha_1^{-1}\alpha_4}{\beta_2\beta_3}, m_4+m_2+l, m_2 + m_4+l, m_2+l+1-j, \beta_2\alpha_1\alpha_2, 0, \beta_2\beta_3\alpha_1, \alpha_4, 0, 0\right) \times \frac{C_l^j\alpha_2^{m_2}\alpha_4^{m_4}}{j!\,\beta_2^{m_4}\,\beta_3^{m_4+m_2}\alpha_1^{m_4}\Gamma(m_2)\Gamma(m_4)}\Gamma(m_4+j) \times\Gamma(m_2+m_4+l) - \sum_{k=0}^{m_3-1}\sum_{n=0}^{k}\sum_{j=0}^{m_1-1}\sum_{l=0}^{j}\frac{C_n^kC_l^j}{k!\,j!\,\alpha_3^{m_7+n-k}} \times \frac{\alpha_1^{-m_4}\alpha_2^{m_2}\alpha_4^{m_4}\alpha_7^{m_7}}{\beta_2^{m_4+m_7+n-k}\beta_3^{m_2+m_4+m_7}\Gamma(m_2)\Gamma(m_4)\Gamma(m_7)}$$

$$\times \Gamma(m_2+m_4+l)\Gamma(m_4+j)\Gamma(m_7+n)\left[\sum_{t=1}^{m_7+n}\kappa_{nt}\right.$$
$$\times T\left(\beta+\alpha_3\beta_2, m_2+l+k-\frac{1}{2}, \frac{\alpha_7\alpha_3^{-1}}{\beta_2\beta_3}, t, m_2+m_4+l, m_2\right.$$
$$\left.+l+1-j, \beta_2\alpha_1\alpha_2, 0, \beta_2\beta_3\alpha_1, \alpha_4, 0, 0\right)+\sum_{v=1}^{m_4+m_2+l}\chi_{lv}$$
$$\times T\left(\beta+\alpha_3\beta_2, m_2+l+k-\frac{1}{2}, \frac{\alpha_1^{-1}\alpha_4}{\beta_2\beta_3}, k, m_2+m_4+l, m_2\right.$$
$$\left.\left.\left.+\ l+1-j, \beta_2\alpha_1\alpha_2, 0, \beta_2\beta_3\alpha_1, \alpha_4, 0, 0\right)\right]\right\} \tag{93}$$

Similarly, by substituting (61) into (90) and then applying ([13], Eq. (3.381.4)) and ([13], Eq. (6.621.3)) to solve the resulting integrals, we obtain $P_{p,e}^{(3,1)}$ of the PN in Scenario 3-Case 1 as

$$P_{p,e}^{(3,1)}$$
$$=\frac{\alpha}{2}-\sum_{i=0}^{m_3-1}\frac{\alpha\alpha_2^{m_2}\alpha_3^i\beta_2^i\Gamma\left(i+\frac{1}{2}\right)}{i!\,\pi^{\frac{1}{2}}\beta^{-\frac{1}{2}}(\alpha_3\beta_2+\beta)^{i+\frac{1}{2}}}-\sum_{j=0}^{m_1-1}\sum_{l=0}^{j}\sum_{k=0}^{m_2-1}\frac{C_l^jC_k^{m_2-1}4^{k+l-j+1}}{j!\,\alpha_1^{-k-l-1}}$$
$$\times\frac{\beta^{\frac{1}{2}}\alpha\beta_2^{m_2+k+l+1}\Gamma\left(m_2+k+l+\frac{3}{2}\right)}{\left[(\alpha_1+\alpha_2+2\sqrt{\alpha_1\alpha_2})\beta_2+b\right]^{m_2+k+l+\frac{3}{2}}}\frac{\Gamma\left(m_2+2j-k-l-\frac{1}{2}\right)}{\Gamma(m_2)\Gamma(m_2+j+1)}$$
$$\times\ {}_2F_1\left(m_2+k+l+\frac{3}{2}, k+l-j+\frac{3}{2}; m_2+j+1; \frac{\left(\alpha_1+\alpha_2-2\sqrt{\alpha_1\alpha_2}\right)\beta_2+\beta}{(\alpha_1+\alpha_2+2\sqrt{\alpha_1\alpha_2})\beta_2+\beta}\right)$$
$$+\sum_{j=0}^{m_1-1}\sum_{l=0}^{j}\sum_{k=0}^{m_2-1}\sum_{i=0}^{m_3-1}\frac{C_l^jC_k^{m_2-1}4^{k+l-j+1}\alpha\alpha_1^{k+l+1}\alpha_2^{m_2}\alpha_3^i}{i!\,j!\,\beta^{-\frac{1}{2}}\beta_2\Gamma(m_2+i+j+1)\Gamma(m_2)}$$
$$\times\frac{\Gamma\left(m_2+i+k+l+\frac{3}{2}\right)\Gamma\left(m_2+i+2j-k-l-\frac{1}{2}\right)}{\left[(\alpha_1+\alpha_2+\alpha_3+2\sqrt{\alpha_1\alpha_2})+\beta\beta_2^{-1}\right]^{m_2+i+k+l+\frac{3}{2}}}$$
$$\times\ {}_2F_1\left(m_2+i+k+l+\frac{3}{2}, k+l-j+\frac{3}{2}; m_2+i+j+1;\right.$$
$$\left.\frac{(\alpha_1+\alpha_2+\alpha_3-2\sqrt{\alpha_1\alpha_2})\beta_2+\beta}{(\alpha_1+\alpha_2+\alpha_3+2\sqrt{\alpha_1\alpha_2})\beta_2+\beta}\right) \tag{94}$$

By substituting (9), (36), (48), (92), (93), and (94) into (91), we obtain the SER of the PN.

5.2 Symbol error rate of the CCRN

According to (55), the SER for the secondary network is given by

$$P_{s,e}=\frac{p_s^{(1,1)}P_{s,e}^{(1,1)}+p_s^{(1,2)}P_{s,e}^{(1,2)}+p_s^{(2,1)}P_{s,e}^{(2,1)}+p_s^{(2,2)}P_{s,e}^{(2,2)}}{p_s} \tag{95}$$

where $P_{s,e}^{(i,j)}$ is the SER of the CCRN in Scenario i-Case j. Substituting (70) into (90), we obtain $P_{s,e}^{(1,1)}$ of the CCRN in Scenario 1-Case 1 as in (96).

$$P_{s,e}^{(1,1)}$$
$$=\frac{\alpha}{2}-\frac{\alpha\sqrt{\beta}}{2\sqrt{\pi}}\sum_{i=0}^{m_6-1}\sum_{j=0}^{i}\frac{C_j^i\Gamma(m_8+j)\Gamma(m_7+i)\alpha_7^{m_7}\alpha_8^{m_7+i-j}\beta_1^{m_7}}{i!\,\Gamma(m_7)\Gamma(m_8)\alpha_6^{m_7}\beta_2^{j-i}}$$
$$\times T\left(\beta, -m_7-\frac{1}{2}, 0, 0, m_7+i, m_7+i+1-m_8-j, \alpha_8\beta_2, \frac{\alpha_7\alpha_8}{\alpha_6\beta_1^{-1}}, 1, 0, 0, 0\right)$$
$$-\frac{\alpha\sqrt{\beta}}{2\sqrt{\pi}}\sum_{p=0}^{m_4-1}\sum_{q=0}^{m_5-1}\frac{\Gamma(m_2+q)\Gamma(m_1+p)\Gamma(m_7+p)}{p!\,q!\,\Gamma(m_1)\Gamma(m_2)\Gamma(m_7)}\frac{\alpha_2^{m_2}\alpha_7^{m_7}\beta_1^{m_7+m_2}}{\alpha_1^{-m_7}\alpha_4^{m_7}\alpha_5^{m_2}\beta_2^{m_2}}$$
$$\times T\left(\beta, -m_7+q-\frac{1}{2}, \frac{\alpha_2\beta_1}{\alpha_5\beta_2}, m_2+q, m_7+p, m_7+1-m_1, 0, \alpha_1\alpha_7\beta_1, \alpha_4, 0, 0, 0\right)$$
$$+\frac{\alpha\sqrt{\beta}}{2\sqrt{\pi}}\sum_{p=0}^{m_4-1}\sum_{q=0}^{m_5-1}\sum_{i=0}^{m_6-1}\sum_{j=0}^{i}\frac{C_j^i\Gamma(m_2+q)\Gamma(m_1+p)}{p!\,q!\,i!\,\Gamma(m_1)\Gamma(m_2)\Gamma(m_7)}$$
$$\times\frac{\Gamma(m_8+j)\Gamma(m_7+p+i)\alpha_1^{m_1}\alpha_2^{m_2}\alpha_7^{m_7}\alpha_8^{m_8}}{\Gamma(m_8)\alpha_4^{m_1}\alpha_5^{m_2}\alpha_6^{m_8+j-i}\beta_1^{i-m_1-m_2-m_8-j}\beta_2^{m_2-i+j}}$$
$$\times\left[\sum_{l=1}^{m_8+j}\kappa_{jl}\left(\frac{\alpha_8\beta_1}{\alpha_6}\right)^{m_7+p+i-l}T\left(\beta, -m_1-m_7-m_8-p+l-j-\frac{1}{2}+q, \frac{\alpha_2\beta_1}{\alpha_5\beta_2}, m_2\right.\right.$$
$$\left.+\ q, m_7+p+i, m_7+p+i+1-l, \alpha_8\beta_2, \frac{\alpha_7\alpha_8}{\alpha_6\beta_1^{-1}}, 1, 0, 0, 0\right)$$
$$+\sum_{k=1}^{m_1+p}\chi_{pk}\left(\frac{\alpha_1\beta_1}{\alpha_4}\right)^{m_7+p+i-k}T\left(\beta, -m_1-m_7-m_8-p+k, -j-\frac{1}{2}+q, \alpha_2\beta_1\alpha_5^{-1}\right.$$
$$\left.\left.\times\ \beta_2^{-1}, m_2+q, m_7+p+i, m_7+p+i+1-k, \alpha_1\alpha_6\beta_2\alpha_4^{-1}, \alpha_1\alpha_7\beta_1\alpha_4^{-1}, 1, 0, 0, 0\right)\right] \tag{96}$$

Furthermore, substituting (73) into (90) together with the help of ([13], Eq. (3.381.4)) and ([17], Eq. (2.3 .6.9)) to solve the resulting integral, we obtain the SER of the CCRN in Scenario 1-Case 2 as

$$P_{s,e}^{(1,2)}=\frac{\alpha}{2}-\sum_{i=0}^{m_6-1}\frac{\alpha\sqrt{\beta\beta_1\alpha_7}\Gamma(m_7+i)}{2i!\sqrt{\pi\alpha_6\beta_2}\Gamma(m_7)}\Gamma\left(i+\frac{1}{2}\right)$$
$$\times U\left(i+\frac{1}{2}, \frac{3}{2}-m_7, \beta\frac{\alpha_7\beta_1}{\alpha_6\beta_2}\right)-\frac{\alpha\sqrt{\beta}}{2\sqrt{\pi}}\sum_{j=0}^{m_4-1}\sum_{k=0}^{m_5-1}\frac{1}{j!\,k!}$$
$$\times\frac{1}{j!\,k!}\frac{1}{\beta_2^{m_2+m_7}\alpha_4^{m_7}\alpha_5^{m_2}\Gamma(m_2)\Gamma(m_7)}$$
$$\times\Gamma(m_2+k)\Gamma(m_7+j)\beta_1^{m_2+m_7}\alpha_2^{m_2}\alpha_7^{m_7}\ \Gamma\left(j+k+\frac{1}{2}\right)$$
$$\times\left[\sum_{l=1}^{m_7+j}\kappa_{jl}\left(\frac{\beta_1\alpha_7}{\beta_2\alpha_4}\right)^{j+k+\frac{1}{2}-l}U\left(j+k+\frac{1}{2}, j+k+\frac{3}{2}-l, \beta\frac{\beta_1\alpha_7}{\beta_2\alpha_4}\right)\right.$$
$$+\sum_{m=1}^{m_2+k}\chi_{km}\left(\frac{\alpha_2\beta_1}{\alpha_5\beta_2}\right)^{j+k+\frac{1}{2}-m}$$
$$\left.\times U\left(j+k+\frac{1}{2}, j+k+\frac{3}{2}-m, \beta\frac{\alpha_2\beta_1}{\alpha_5\beta_2}\right)\right]+\frac{\alpha\sqrt{\beta}}{2\sqrt{\pi}}\sum_{i=0}^{m_6-1}\sum_{j=0}^{m_4-1}\sum_{k=0}^{m_5-1}$$

$$\times \frac{\beta_1^{m_2+m_7}\alpha_2^{m_2}\alpha_4^{j}\alpha_6^{i}\alpha_7^{m_7}\Gamma\left(i+j+k+\frac{1}{2}\right)}{j!\,k!\,k!\,\beta_2^{m_2+m_7}\alpha_5^{m_2}(\alpha_4+\alpha_6)^{(m_7+i+j)}}$$
$$\times \frac{\Gamma(m_2+k)\Gamma(m_7+i+j)}{\Gamma(m_2)\Gamma(m_7)}\left[\sum_{n=1}^{m_7+k}\xi_{kn}\left(\frac{\alpha_2\beta_1}{\alpha_5\beta_2}\right)^{i+j+k+\frac{1}{2}-n}\right.$$
$$\times U\left(i+j+k+\frac{1}{2}, i+j+k+\frac{3}{2}-n, \beta\frac{\alpha_2\beta_1}{\alpha_5\beta_2}\right)$$
$$+\sum_{t=1}^{m_7+i+j}\theta_{ijt}\left(\frac{\alpha_7\beta_1}{\alpha_4\beta_2+\alpha_6\beta_2}\right)^{i+j+k+\frac{1}{2}-t}$$
$$\left.\times U\left(i+j+k+\frac{1}{2}, i+j+k+\frac{3}{2}-t, \frac{\beta\alpha_7\beta_1\beta_2^{-1}}{\alpha_4+\alpha_6}\right)\right] \tag{97}$$

Similarly, the SER of the CCRN in Scenario 2-Case 2 can be derived by substituting (74) into (90) and utilizing ([13], Eq. (3.381.4)) and ([17], Eq. (2.3 .6.9)) to solve the resulting integral as

$$P_{s,e}^{(2,2)} = \frac{\alpha}{2} - \sum_{i=0}^{m_6-1}\sum_{j=0}^{i}\sqrt{\frac{\beta\beta_2\beta_3}{\pi\alpha_8^{-1}\alpha_6}}\frac{\alpha C_j^i\alpha_8{}^{m_8}\Gamma(m_8+j)}{2i!\,\beta_2^{j-i}\Gamma(m_8)}\Gamma\left(i+\frac{1}{2}\right)$$
$$\times U\left(i+\frac{1}{2}, i+\frac{3}{2}-m_8-j, \frac{\alpha_6+\beta_3\beta}{\alpha_6\alpha_8^{-1}\beta_2^{-1}}\right)$$
$$-\frac{\alpha\sqrt{\beta}}{2\sqrt{\pi}}\sum_{p=0}^{m_4-1}\sum_{q=0}^{m_5-1}\frac{\alpha_5^q\Gamma(m_1+p)}{p!\,q!\,\beta_3^q\Gamma(m_1)}\Gamma\left(p+q+\frac{1}{2}\right)\left(\frac{\beta_2\beta_3}{\alpha_1^{-1}\alpha_4}\right)^{q+\frac{1}{2}}$$
$$\times U\left(p+q+\frac{1}{2}, q+\frac{3}{2}-m_1, \frac{\alpha_5+\beta_3\beta}{\alpha_1^{-1}\alpha_4\beta_2^{-1}}\right)+\frac{\alpha\sqrt{\beta}}{2\sqrt{\pi}}\sum_{i=0}^{m_6-1}\sum_{j=0}^{i}\sum_{p=0}^{m_4-1}\sum_{q=0}^{m_5-1}$$
$$\frac{C_j^i\alpha_1^{m_1}\alpha_5^q\alpha_8^{m_8}\beta_2{}^{m_1+m_8}\Gamma(m_1+p)\Gamma(m_8+j)}{i!\,p!\,q!\,\alpha_4{}^{m_1}\alpha_6^{m_8+j-i}\beta_3^{i+q-m_1-m_8-j}\Gamma(m_1)\Gamma(m_8)}\Gamma\left(i+p+q+\frac{1}{2}\right)$$
$$\times\left[\sum_{l=1}^{m_8+j}\mu_{lj}\left(\frac{\beta_2\beta_3}{\alpha_6\alpha_8^{-1}}\right)^{i+p+q+\frac{1}{2}-l}\right.$$
$$\times U\left(i+p+q+\frac{1}{2}, i+p+q+\frac{3}{2}-l, \frac{\alpha_5+\alpha_6+\beta\beta_3}{\alpha_6\alpha_8^{-1}\beta_2^{-1}}\right)$$
$$+\sum_{k=1}^{m_1+p}\eta_{ki}\left(\frac{\alpha_1\beta_2\beta_3}{\alpha_4}\right)^{i+p+q+\frac{1}{2}-k}$$
$$\left.\times U\left(i+p+q+\frac{1}{2}, i+p+q+\frac{3}{2}-k, \frac{\alpha_5+\alpha_6+\beta\beta_3}{\alpha_1^{-1}\alpha_4\beta_2^{-1}}\right)\right] \tag{98}$$

Moreover, substituting (78) into (90) together with the help of ([13], Eq. (3.381.4)) and ([13], Eq. (6.621.3)) to solve the integral, we obtain the SER of the CCRN in Scenario 2-Case 1 as

$$P_{s,e}^{(2,1)} = \frac{\alpha}{2} - \frac{\alpha\sqrt{\beta}}{2\sqrt{\pi}}\sum_{l=0}^{m_6-1}\frac{1}{l!}\frac{\alpha_6^l\beta_3^{\frac{1}{2}}\Gamma\left(l+\frac{1}{2}\right)}{(\alpha_6+\beta\beta_3)^{l+\frac{1}{2}}} - \alpha\sqrt{\beta}\sum_{k=0}^{m_4-1}\sum_{t=0}^{k}\sum_{h=0}^{m_5-1}$$
$$\times\frac{C_t^kC_h^{m_5-1}4^{h+t-k+1}\alpha_4^{h+t+1}\alpha_5^{m_5}\beta_3^{\frac{1}{2}}}{k!\,(\alpha_4+\alpha_5+\beta\beta_3+2\sqrt{\alpha_4\alpha_5})^{m_5+h+t+\frac{3}{2}}}$$
$$\times\frac{\Gamma\left(m_5+h+t+\frac{3}{2}\right)\Gamma\left(m_5+2k-t-h-\frac{1}{2}\right)}{\Gamma(m_5)\Gamma(m_5+k+1)}$$
$$\times{}_2F_1\left(m_5+h+t+\frac{3}{2}, h+t-k+\frac{3}{2}; m_5+k+1;\right.$$
$$\left.\frac{\alpha_4+\alpha_5+\beta\beta_3-2\sqrt{\alpha_4\alpha_5}}{\alpha_4+\alpha_5+\beta\beta_3+2\sqrt{\alpha_4\alpha_5}}\right)+\sum_{k=0}^{m_4-1}\sum_{t=0}^{k}\sum_{h=0}^{m_5-1}\sum_{l=0}^{m_6-1}$$
$$\times\frac{C_t^kC_h^{m_5-1}4^{h+t-k+1}\alpha\alpha_4^{h+t+1}\alpha_5^{m_5}\alpha_6^{l}\Gamma(m_5+2k-t-h-\frac{1}{2})}{k!\,l!\,\beta_3^{l-frac12}\beta^{-\frac{1}{2}}\left(\alpha_4+\alpha_5+\beta\beta_3+2\sqrt{\alpha_4\alpha_5}\right)^{m_5+h+t+\frac{3}{2}}}$$
$$\times\frac{\Gamma(m_5+h+t+\frac{3}{2})}{\Gamma(m_5)\Gamma(m_5+k+1)}{}_2F_1\left(m_5+h+t+\frac{3}{2}, h+t-k+\frac{3}{2}; m_5+k+1;\right.$$
$$\left.\frac{\alpha_4+\alpha_5+\beta\beta_3-2\sqrt{\alpha_4\alpha_5}}{\alpha_4+\alpha_5+\beta\beta_3+2\sqrt{\alpha_4\alpha_5}}\right) \tag{99}$$

Finally, substituting (9), (21), (29), (36), (96), (97), (98), and (99) into (95), the SER of the CCRN can be found.

6 Numerical results

In this section, we present numerical results to evaluate the performance for the PN and the CCRN for various network parameters. In particular, the numerical results are provided to quantify the considered metrics and to illustrate the performance improvement obtained when applying the proposed relaying-assisted hybrid spectrum access scheme.

Let us recall that $d_1, d_2, d_3, d_4, d_5, d_6, d_7$, and d_8 denote the normalized distances of the links $\mathrm{PU_{TX}} \rightarrow \mathrm{SU_R}$, $\mathrm{SU_R} \rightarrow \mathrm{PU_{RX}}, \mathrm{PU_{TX}} \rightarrow \mathrm{PU_{RX}}, \mathrm{SU_{TX}} \rightarrow \mathrm{SU_R}, \mathrm{SU_R} \rightarrow \mathrm{SU_{RX}}, \mathrm{SU_{TX}} \rightarrow \mathrm{SU_{RX}}, \mathrm{SU_{TX}} \rightarrow \mathrm{PU_{RX}}$, and $\mathrm{PU_{TX}} \rightarrow \mathrm{SU_{RX}}$, respectively. Assume that the considered system operates in a suburban environment such that all channel mean powers are attenuated with the link distances according to the exponential decaying path loss model with path loss exponent of 4. The SINR threshold used for calculating the outage probability is selected as $\gamma_{\mathrm{th}} = 3$ dB. Further, the expected outage threshold is chosen as $\epsilon = 0.1$ % when calculating the outage capacity.

First, we will illustrate the impact of imperfect spectrum sensing at the SUs, the fading severity parameters, and the communication link distances d_1, d_2, and d_3 of the PN on the system performance in terms of outage probability, outage capacity, and SER of the PN. To reveal the superior performance of the proposed scheme, we then provide a comparison of the performance of the PN with and without the use of the secondary relay. Assume that the arrival processes of the PN and CCRN follow a Poisson distribution with arrival rates $\lambda_p = \lambda_s = 85$ packets/sec.

Furthermore, the departure processes of the PN and secondary network at SU_{TX} and PU_{TX} are also modeled as Poisson distribution with rate $\mu_s = \mu_p = 100$ packets/sec. Moreover, departure rates at SU_R for the traffics from the primary transmitter and secondary transmitter are set as $\mu_r^s = \mu_r^p = 100$ packets/s. In addition, the so-called transmit signal-to-noise ratio (SNR) of the CCRN in the interweave mode and the interference-power-to-noise ratio in the underlay mode are selected as $P_s/N_0 = 10$ dB and $Q/N_0 = 5$ dB, respectively. Finally, the distances, d_4, d_5, d_6, associated with the communication links and the distances, d_7, d_8, associated with the interference links of the CCRN are fixed as $d_4 = d_5 = 0.6$, $d_6 = 1.2$, and $d_7 = d_8 = 0.9$.

Figure 3a–c depicts the outage probability, outage capacity, and SER of the PN versus false alarm probability p_f and missed detection probability p_m of the SUs for the case that $p_f = p_m$. The transmit SNR of the PN is chosen as $P_p/N_0 = 10$ dB. In addition, the communication link distances of the PN are fixed at $d_1 = d_2 = 0.4, d_3 = 0.6$. Furthermore, the following cases of fading severity parameters are selected:

- Case 1: $(m_1, m_2, m_3, m_4, m_5, m_6, m_7, m_8) = (3, 3, 3, 3, 3, 3, 3, 3)$
- Case 2: $(m_1, m_2, m_3, m_4, m_5, m_6, m_7, m_8) = (2, 2, 2, 2, 2, 2, 2, 2)$
- Case 3: $(m_1, m_2, m_3, m_4, m_5, m_6, m_7, m_8) = (2, 2, 2, 2, 2, 2, 1, 1)$

As can be seen from Fig. 3a–c, Case 1 provides the lowest outage probability and SER, and the highest outage capacity as compared to Cases 2 and 3 because Case 1 has more favorable fading conditions. Furthermore, Case 3 considers different fading severity parameters on different channels. Specifically, Rayleigh fading is present on the interference channels from the secondary transmitter to the primary receiver and from the primary transmitter to the secondary receiver, i.e., $m_7 = m_8 = 1$, while the communication channels inside the PN and the CCRN have the some line-of-sight links with $m_i = 2$, $i = 1, 2, \ldots, 6$. As Case 3 induces more severe fading on the interference links compared to Case 2, while communication links in both cases have the same fading severity parameter, a performance improvement in the PN is observed for Case 3. Finally, imperfect spectrum sensing of the SUs degrades the performance of the PN, i.e, the outage probability and SER increase and the outage capacity decreases as the false alarm and missed detection probabilities of the SUs increase.

Figure 4a–c presents comparisons for the outage probability, outage capacity, and SER of the PN with and without the assistance of the secondary relay. For these examples, we assume that the SUs can perform spectrum sensing perfectly. Moreover, the fading severity parameters of all

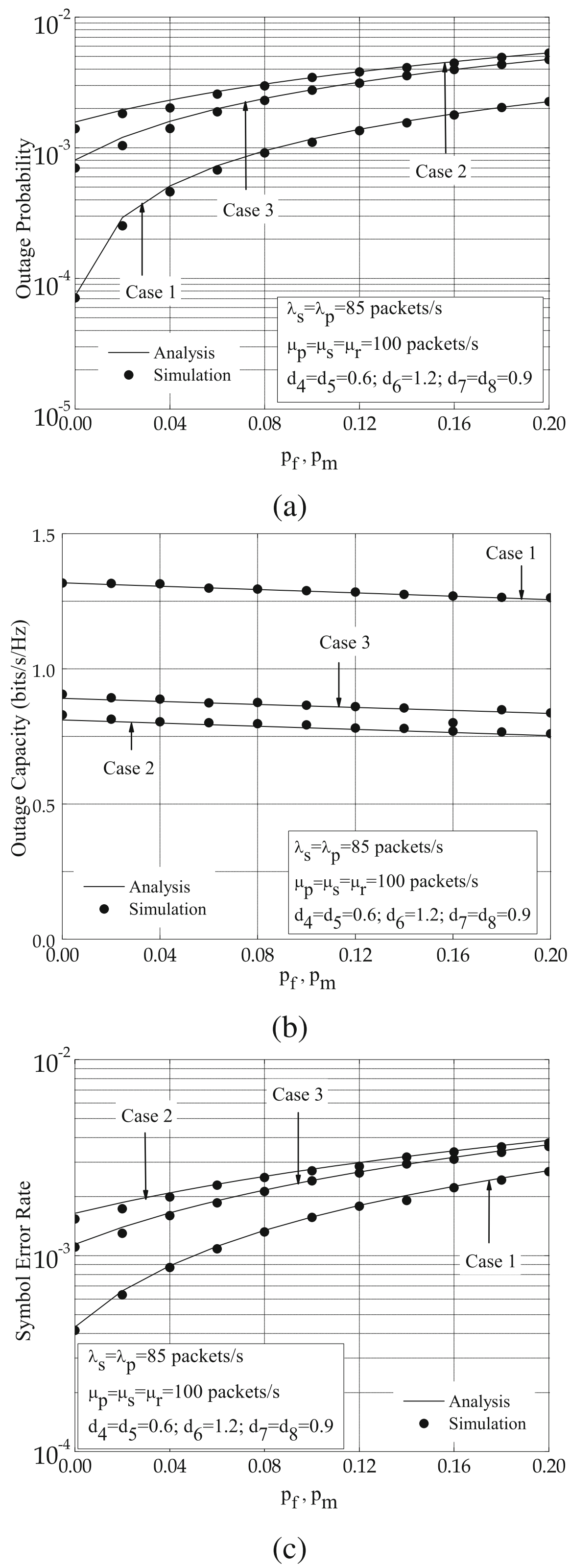

Fig. 3 Performance of the primary network for various fading parameters: **a** outage probability, **b** outage capacity, **c** symbol error rate

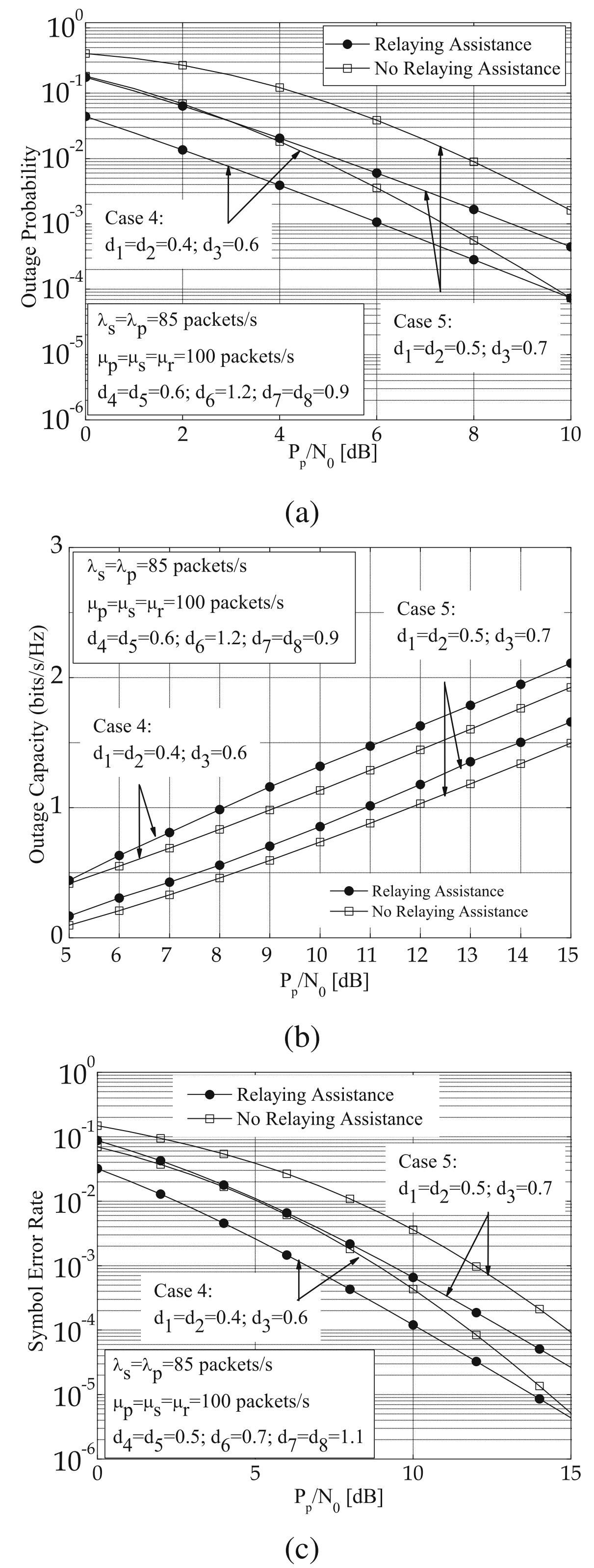

Fig. 4 Performance comparisons of the primary network with and without the assistance of the secondary relay: **a** outage probability, **b** outage capacity, **c** symbol error rate

the links are selected as, $m_i = 3$, $i = 1, 2, \ldots, 8$. Furthermore, the normalized distances in the PN, i.e., d_1 from PU_{TX} to SU_R, d_2 from SU_R to PU_{RX}, and d_3 from PU_{TX} to PU_{RX}, are selected as

- Case 4: $d_1 = d_2 = 0.4$ and $d_3 = 0.6$
- Case 5: $d_1 = d_2 = 0.5$ and $d_3 = 0.7$

As can be seen from Fig. 4a–c, with the communication link distances $d_1 = d_2 = 0.4$ and $d_3 = 0.6$, Case 4 provides lower outage probability and SER, and higher outage capacity as compared to Case 5. This is because all channel mean powers are attenuated with the link distances according to an exponentially decaying function. Thus, the average channel power gains of the communication channels of the PN in Case 4 are higher than those of Case 5. It can also be observed from these figures that the proposed relaying scheme where the relay assists the communication of both the PN and SN can improve the performance of the PN. In particular, with the help of the secondary relay, the outage probability, outage capacity, and SER of the PN always outperform those results obtained for the PN without the assistance of the secondary relay in both Case 4 and Case 5.

Next, we investigate the effect of the arrival rate of the PN and imperfect spectrum sensing of the SUs on the outage probability, outage capacity, and SER of the CCRN. Then, we demonstrate the influence of the transmit SNR P_s/N_0 in interweave mode and the interference-power-to-noise ratio Q/N_0 of PU_{RX} in underlay mode on the performance of the CCRN. In addition, a comparison of the performance of the hybrid interweave-underlay CCRN with that of the conventional underlay CCRN is presented. In these examples, we select the arrival rate of SU_{TX} as $\lambda_s = 85$ packets/s, and the departure rates of PU_{TX}, SU_{TX}, and SU_R as $\mu_p = \mu_s = \mu_r^p = \mu_r^s = 100$ packets/s. The transmit SNR of the PN is selected as $P_p/N_0 = 10$ dB. Furthermore, for these examples, the communication link distances, d_1, d_2, d_3, of the PN and the interference link distances, d_7, d_8, are fixed as $d_1 = d_2 = 0.8$, $d_3 = 1.1$, and $d_7 = d_8 = 1.1$. Finally, the fading severity parameters are chosen to be the same for all links as $m_i = 2$, $i = 1, 2, \ldots, 8$.

Figure 5a–c illustrates the outage probability, outage capacity, and SER of the CCRN versus Q/N_0 for different arrival rates λ_p of the PN:

- Case 6: $\lambda_p = 10$ packets/s
- Case 7: $\lambda_p = 100$ packets/s

For each case, we investigate various levels of imperfect spectrum sensing of the SUs on the performance of the hybrid CCRN, i.e., ($p_f = 0, p_m = 0$) for the case of perfect spectrum sensing, ($p_f = 0, p_m = 0.2$) for the case of 20 % of missed detection, and ($p_f = 0.2, p_m = 0$) for the case of

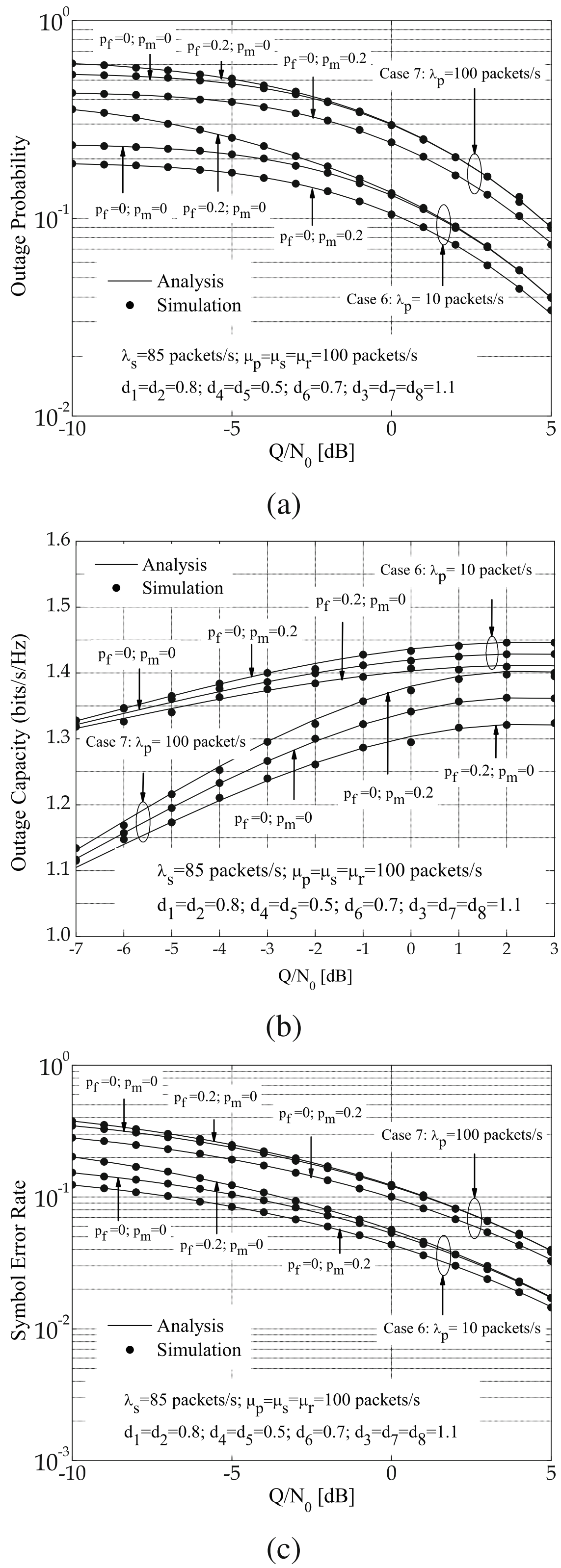

Fig. 5 Performance of the CCRN using the hybrid scheme for different arrival rates of the PN: **a** outage probability, **b** outage capacity, **c** symbol error rate

20 % of false alarm. In these examples, we select the communication link distances of the CCRN as $d_4 = d_5 = 0.5$ and $d_6 = 0.7$. Furthermore, we fix the transmit SNR in the interweave mode as $P_s/N_0 = 10$ dB. As expected, when the arrival rate of the PN decreases from Case 7 to Case 6, the performance of the CCRN improves significantly, i.e., the outage probability and SER decrease and the outage capacity increases. This is attributed to the fact that as λ_p decreases, the idle periods of the PN increases. Thus, the probability that the CCRN operates in the interweave mode increases. It can also be observed that false alarm degrades the performance of the SN since it reduces the opportunity for the SN to operate in the interweave mode. Finally, missed detection increases the chance for the SN to operate in the interweave mode which increases the performance of the SN. However, when missed detection occurs, the SUs assume that the licensed spectrum is vacant although it is occupied by the PUs which degrades the performance of the PN as can be seen in Fig. 3.

Figure 6a–c shows performance comparisons between the hybrid interweave-underlay CCRN and the conventional underlay CCRN in terms of outage probability, outage capacity, and SER. In these examples, it is assumed that the SUs can perform perfect spectrum sensing. Further, we fix the transmit SNR of the CCRN and arrival rate of the PN as $P_s/N_0 = 10$ dB and $\lambda_p = 85$ packets/s, respectively. Then, we investigate the effect of the normalized distances in the CCRN, i.e., d_4 from SU_{TX} to SU_R, d_5 from SU_R to SU_{RX}, and d_6 from SU_{TX} to SU_{RX}, for the following cases:

- Case 8: $d_4 = d_6 = 0.4$ and $d_6 = 0.7$
- Case 9: $d_4 = d_5 = 0.5$ and $d_6 = 0.8$

As expected, when d_4, d_5, and d_6 increase from Case 8 to Case 9, the outage probability and SER of the hybrid CCRN and conventional CCRN increase. However, the outage capacity decreases according to the increase of d_4, d_5, and d_6 since the transmit signals are attenuated with distance according to the exponential decaying path loss model. Finally, for both of the examined cases in Fig. 6, the performance of the proposed hybrid CCRN always outperforms that of the respective underlay CCRN.

7 Conclusions

In this paper, we have utilized a continuous-time Markov chain to model the spectrum access of the PU and SUs of a hybrid interweave-underlay CCRN wherein an AF relay assists both the PN and CCRN. Based on this Markov model, we have obtained the steady state probability of each state which then is utilized to calculate the probability of each scenario of the PN and CCRN. Considering mutual interference between the PN and CCRN, we have derived expressions for the outage probability,

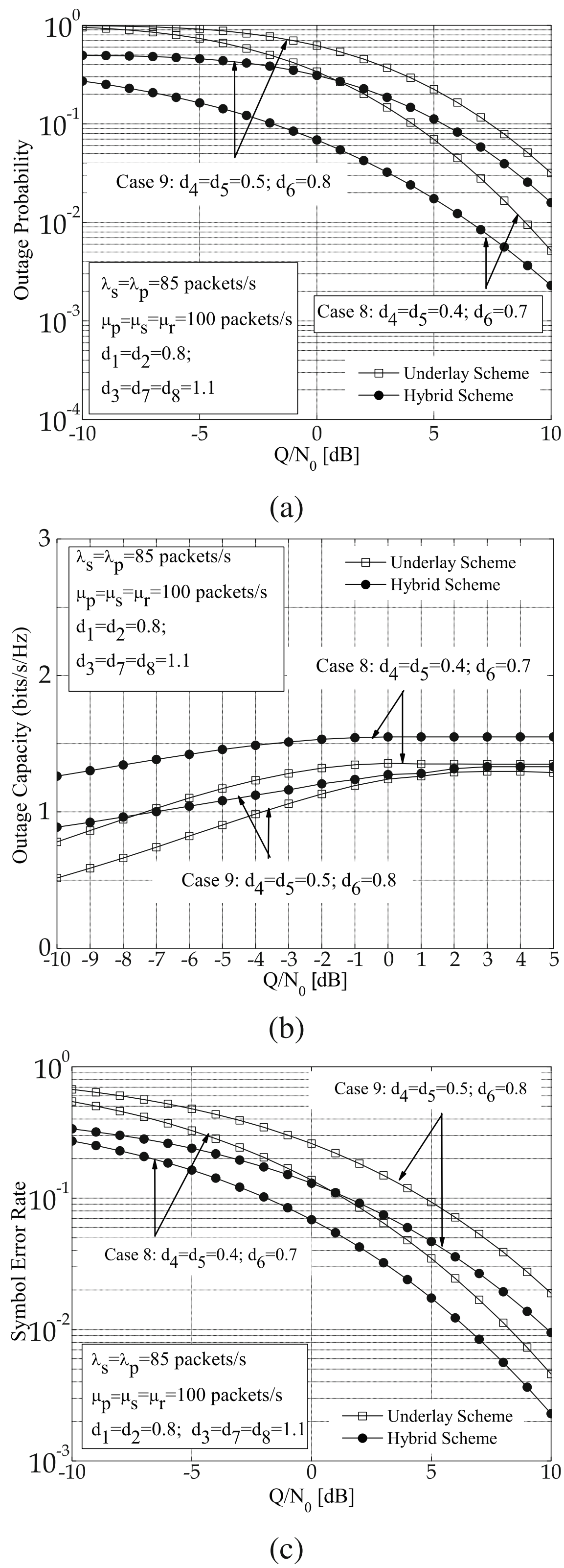

Fig. 6 Performance comparisons of the CCRN when using the underlay and hybrid schemes: **a** outage probability, **b** outage capacity, **c** symbol error rate

outage capacity, and SER for both networks under imperfect spectrum sensing. Numerical results have been provided to illustrate the effect of the primary arrival rates, the fading severity parameters, the communication and interference link distances, and the interference power threshold of PU_{RX} on the performance of the PN and CCRN. Through the selected examples, it can be observed that the PN can achieve a performance improvement with the assistance of the secondary relay to forward its signals. Finally, for the selected numerical results, the performance of the CCRN applying the propose hybrid interweave-underlay spectrum access always outperforms that of the conventional underlay CCRN.

Appendix 1: Proof of Theorem 1

In view of (16) and (17), we see that $\gamma_{1p}^{(1,1)}$ and $\gamma_{2p}^{(1,1)}$ are independent. Based on the order statistics theory, we can derive the CDF for the instantaneous SINR $\gamma_p^{(1,1)}$ of the PN in Scenario 1 from (15) as

$$F_{\gamma_p^{(1,1)}}(\gamma) = F_{\gamma_{1p}^{(1,1)}}(\gamma) F_{\gamma_{2p}^{(1,1)}}(\gamma) \tag{A.1}$$

where $F_{\gamma_{1p}^{(1,1)}}(\gamma)$ and $F_{\gamma_{2p}^{(1,1)}}(\gamma)$ are, respectively, the CDFs of the instantaneous SINRs of the direct and relaying links of the PN in Scenario 1-Case 1. From (16), we can obtained $F_{\gamma_{1p}^{(1,1)}}(\gamma)$ as

$$\begin{aligned} F_{\gamma_{1p}^{(1,1)}}(\gamma) &= F_{X_3}\left(\gamma\left(\beta_1+\beta_2\right)\right) \\ &= 1-\exp\left(-\alpha_3\left(\beta_1+\beta_2\right)\gamma\right)\sum_{p=0}^{m_3-1}\frac{\alpha_3^p\gamma^p\left(\beta_1+\beta_2\right)^p}{p!} \end{aligned} \tag{A.2}$$

Furthermore, the CDF of the instantaneous SINR of the relaying link for the PN in Scenario 1-Case 1 $F_{\gamma_{2p}^{(1,1)}}(\gamma)$ can be calculated from (17) as

$$F_{\gamma_{2p}^{(1,1)}}(\gamma) = \int_0^\infty \left(\int_0^\infty F_{X_1}\left(\frac{\gamma\left(\beta_1+\beta_2\right)x_4}{x_7}\right) f_{X_4}\left(x_4\right)dx_4\right) f_{X_7}\left(x_7\right)dx_7 \tag{A.3}$$

With $f_{X_i}(x_i)$ in (1) and $F_{X_i}(x_i)$ in (2) together with the help of ([13], Eq. (3.381.4)), after some algebraic modifications, we can write $F_{\gamma_{2p}^{(1,1)}}(\gamma)$ as

$$\begin{aligned} F_{\gamma_{2p}^{(1,1)}}(\gamma) =& 1-\sum_{q=0}^{m_1-1}\frac{\alpha_1^q\alpha_7^{m_7}\gamma^q(\beta_1+\beta_2)^q\Gamma(m_4+q)}{q!\,\alpha_4^q\Gamma(m_7)\Gamma(m_4)} \\ &\times\int_0^\infty\frac{x_7^{m_4+m_7-1}}{\left(x_7+\frac{\alpha_1\gamma(\beta_1+\beta_2)}{\alpha_4}\right)^{m_4+q}}\exp(-\alpha_7x_7)dx_7 \end{aligned} \tag{A.4}$$

Using ([17], Eq. (2.3 .6 .9)) to calculate the remaining integral, we obtain $F_{\gamma_{2p}^{(1,1)}}(\gamma)$ as

$$F_{\gamma_{2p}^{(1,1)}}(\gamma)=1-\sum_{q=0}^{m_1-1}\frac{\alpha_1^{m_7}\alpha_7{}^{m_7}\gamma^{m_7}\left(\beta_1+\beta_2\right)^{m_7}}{q!\,\alpha_4^{m_7}}\frac{\Gamma\left(m_4+q\right)\Gamma\left(m_4+m_7\right)}{\Gamma\left(m_7\right)\Gamma\left(m_4\right)} \times U\left(m_4+m_7,m_7+1-q,\frac{\alpha_1\alpha_7\gamma\left(\beta_1+\beta_2\right)}{\alpha_4}\right) \tag{A.5}$$

Finally, substituting (A.2) and (A.5) into (A.1), we obtain $F_{\gamma_p^{(1,1)}}(\gamma)$ as in (57).

Appendix 2: Proof of Theorem 2

Utilizing the order statistics theory along with the total probability theorem, the instantaneous SINR of the PN in Scenario 2-Case 2 is calculated from (42) as

$$F_{\gamma_p^{(2,2)}}(\gamma)=F_{\gamma_{1p}^{(2,2)}}(\gamma)F_{\gamma_{2p}^{(2,2)}}(\gamma) \tag{B.1}$$

where $F_{\gamma_{1p}^{(2,2)}}(\gamma)$ and $F_{\gamma_{2p}^{(2,2)}}(\gamma)$ are, respectively, the instantaneous SINRs of the direct and relaying links of the PN in Scenario 2-Case 2. From (2) and (43) together with the help of ([13], Eq. (3.381.4)), we can obtain $F_{\gamma_{1p}^{(2,2)}}(\gamma)$ as

$$F_{\gamma_{1p}^{(2,2)}}(\gamma)=1-\sum_{k=0}^{m_3-1}\sum_{n=0}^{k}\frac{C_n^k\beta_3{}^n\alpha_3^k\alpha_7{}^{m_7}\beta_2{}^k\Gamma\left(m_7+n\right)\gamma^k}{k!\,\Gamma\left(m_7\right)\left(\alpha_3\gamma\beta_2\beta_3+\alpha_7\right)^{(m_7+n)}} \times\exp\left(-\alpha_3\gamma\beta_2\right) \tag{B.2}$$

Further, an expression of $F_{\gamma_{1p}^{(2,2)}}(\gamma)$ can be derived from (44) as

$$F_{\gamma_{2p}^{(2,2)}}(\gamma)=\int_0^\infty\left[\int_0^\infty F_{X_1}\left(\frac{\gamma\beta_2\beta_3x_2x_4+\gamma\beta_2x_4}{x_2}\right)f_{X_4}(x_2)\,dx_4\right]f_{X_2}(x_2)dx_2 \tag{B.3}$$

Substituting (1) and (2) into (B.3) and then utilizing ([13], Eq. (3.381.4)) and ([17], Eq. (2.3.6.9)) to solve the resulting integrals, we obtain $F_{\gamma_{2p}^{(2,2)}}(\gamma)$ as

$$F_{\gamma_{2p}^{(2,2)}}(\gamma)=1-\sum_{j=0}^{m_1-1}\sum_{l=0}^{j}\frac{C_l^j\alpha_2{}^{m_2}\alpha_4{}^{m_4}}{j!\,\beta_2{}^{m_4}\beta_3{}^{m_4+m_2}\alpha_1{}^{m_4}} \times\frac{\Gamma(m_4+j)\Gamma(m_2+m_4+l)}{\Gamma(m_2)\Gamma(m_4)}\frac{\gamma^{m_2+l}}{\left(\gamma+\frac{\alpha_4}{\beta_2\beta_3\alpha_1}\right)^{m_4+m_2+l}} \times U\left(m_2+m_4+l,m_2+l+1-j,\frac{\gamma\beta_2\alpha_1\alpha_2}{\gamma\beta_2\beta_3\alpha_1+\alpha_4}\right) \tag{B.4}$$

Finally, substituting (B.2) and (B.4) into (B.1), after some algebraic manipulations, the CDF of $\gamma_p^{(2,2)}$ can be derived as in (58).

Appendix 3: Proof of Theorem 3

From (52), the instantaneous SINR of the PN in Scenario 3-Case 1 is calculated as

$$F_{\gamma_p^{(3,1)}}(\gamma)=F_{\gamma_{1p}^{(3,1)}}(\gamma)F_{\gamma_{2p}^{(3,1)}}(\gamma) \tag{C.1}$$

where $F_{\gamma_{1p}^{(1,2)}}(\gamma)$ is the instantaneous SINR of the direct link of the PN in Scenario 3-Case 1 which can be obtained from (53) and (2) as

$$F_{\gamma_{1p}^{(3,1)}}(\gamma)=1-\exp\left(-\alpha_3\beta_2\gamma\right)\sum_{l=0}^{m_3-1}\frac{\alpha_3^l\beta_2{}^l\gamma^l}{l!} \tag{C.2}$$

Further, $F_{\gamma_{2p}^{(1,2)}}(\gamma)$ is the instantaneous SINR of the relaying link of the PN in Scenario 3-Case 1 which can be derived from (54) as

$$F_{\gamma_{2p}^{(3,1)}}(\gamma)=\int_0^{\gamma\beta_2}f_{X_2}(x_2)dx_2+\int_{\gamma\beta_2}^\infty F_{X_1}\left(\frac{\beta_2\gamma x_2}{x_2-\gamma\beta_2}\right)f_{X_2}(x_2)dx_2 \tag{C.3}$$

Substituting (2) and (1) into (C.3) together with the help of ([13], Eq. (3.471 .9)), we obtain $F_{\gamma_{1p}^{(1,2)}}(\gamma)$ as

$$F_{\gamma_{2p}^{(3,1)}}(\gamma)=1-2\sum_{j=0}^{m_1-1}\sum_{l=0}^{j}\sum_{k=0}^{m_2-1}\frac{C_l^jC_k^{m_2-1}\gamma^{m_2+j}}{j!\,\Gamma(m_2)} \times\frac{\beta_2^{m_2+j}\exp(-(\alpha_1+\alpha_2)\beta_2\gamma)}{\alpha_2^{\frac{-2m_2+k+l-j+1}{2}}\alpha_1^{\frac{-k-l-j-1}{2}}} \times\mathcal{K}_{k+l-j+1}(2\sqrt{\alpha_1\alpha_2}\gamma\beta_2) \tag{C.4}$$

By substituting (C.2) and (C.4) into (C.1), we finally obtain the CDF of $\gamma_p^{(2,2)}$ as in (61).

Competing interests

The authors declare that they have no competing interests.

Author details

[1]Blekinge Institute of Technology, SE-371 79 Karlskrona, Sweden. [2]University of Reading, RG6 6AY Reading, UK.

Received: 2 February 2016 Accepted: 17 August 2016
Published online: 12 October 2016

References

1. MA McHenry, *Spectrum white space measurements*, Presentation to New America Foundation Broadband Forum, (Washington DC, 2003). http://www.newamerica.net/Download_Docs/pdfs/Doc_File_185_1.pdf
2. VA Bohara, SH Ting, Y Han, A Pandharipande, in *Proc. Cognitive Radio Oriented Wireless Networks Communications*. Interference-free overlay cognitive radio network based on cooperative space time coding, (Cannes, 2010), pp. 1–5
3. R Zhang, On peak versus average interference power constraints for protecting primary users in cognitive radio networks. IEEE Trans. Wireless Commun. **8**(4), 2112–2120 (2009)
4. S Haykin, Cognitive radio: brain-empowered wireless communications. IEEE J. Sel. Areas in Commun. **23**(2), 201–220 (2005)
5. L Giupponi, C Ibars, in *Proc. IEEE Veh. Technol. Conf. - Spring*. Distributed cooperation in cognitive radio networks: overlay versus underlay paradigm (IEEE, Barcelona, 2009), pp. 1–6

6. J Oh, W Choi, in *Proc. IEEE Veh. Technol. Conf. -Fall*. A hybrid cognitive radio system: a combination of underlay and overlay approaches (IEEE, Ottawa, 2010), pp. 1–5
7. KBS Manosha, N Rajatheva, M Latva-aho, in *Proc. IEEE Veh. Technol. Conf. - Spring*. Overlay/underlay spectrum sharing for multi-operator environment in cognitive radio networks (IEEE, Budapest, 2011), pp. 1–5
8. J Zou, H Xiong, D Wang, CW Chen, Optimal power allocation for hybrid overlay/underlay spectrum sharing in multiband cognitive radio networks. IEEE Trans. Veh. Technol. **62**(4), 1827–1837 (2013)
9. Z Yan, X Zhang, W Wang, in *Proc. IEEE Wireless Commun. Networking Conf.* Outage performance of relay assisted hybrid overlay/underlay cognitive radio systems (IEEE, Quintana Roo, 2011), pp. 1920–1925
10. J Hu, LL Yang, L Hanzo, in *Proc. IEEE Global Commun. Conf.* Optimal queue scheduling for hybrid cognitive radio maintaining maximum average service rate under delay constraint (IEEE, Anaheim, 2012), pp. 1398–1403
11. TMC Chu, H Phan, HJ Zepernick, Hybrid interweave-underlay spectrum access for cognitive cooperative radio networks. IEEE Trans. Commun. **62**(7), 2183–2197 (2014)
12. TMC Chu, H Phan, HJ Zepernick, in *Proc. IEEE Int. Symp. on Personal, Indoor and Mobile Radio Commun*. Amplify-and-forward relay assisting both primary and secondary transmissions in cognitive radio networks over Nakagami-m fading (IEEE, Sydney, 2012), pp. 954–959
13. IS Gradshteyn, IM Ryzhik, *Table of Integrals, Series, and Products 7th ed*. (Academic Press, San Diego, 2007)
14. TMC Chu, H Phan, HJ Zepernick, Performance analysis of MIMO cognitive amplify-and-forward relay networks with orthogonal space-time block codes. Wirel. Commun. Mob. Comput (2014). doi:10.1002/wcm.2449
15. C Zhong, S Jin, KK Wong, Dual-hop systems with noisy relay and interference-limited destination. IEEE Trans. Commun. **58**(3), 764–768 (2010)
16. B Wang, Z Ji, KJR Liu, T Clancy, Primary-prioritized Markov approach for dynamic spectrum allocation. IEEE Trans. Wireless Commun. **8**(4), 1854–1865 (2009)
17. AP Prudnikov, YA Brychkov, OI Marichev, *Integrals and Series*, vol. 1. (Gordon and Breach Science Publishers, New York, 1986)
18. J Perez, J Ibanez, L Vielva, L Santamaria, Closed-form approximation for the outage capacity of orthogonal STBC. IEEE Commun. Lett. **9**(11), 961–963 (2005)
19. RHY Louie, Y Li, HA Suraweera, B Vucetic, Performance analysis of beamforming in two hop amplify and forward relay networks with antenna correlation. IEEE Trans. Wireless Commun. **8**(6), 3132–3141 (2009)